2020

Effects on Initial Fixation of Cementless Tibial Trays in Total Knee Arthroplasty

Brooke Fritts Thompson

Effects on Initial Fixation of Cementless Tibial Trays in Total Knee Arthroplasty

A Thesis

Presented to

the Faculty of the Daniel Felix Ritchie School of Engineering and Computer Science

University of Denver

In Partial Fulfillment

of the Requirements for the Degree

Master of Science

by

Brooke Fritts Thompson

August 2020

Advisor: Dr. Chadd W. Clary, PhD

Author: Brooke Fritts Thompson
Title: Effects on Initial Fixation of Cementless Tibial Trays in Total Knee Arthroplasty
Advisor: Dr. Chadd Clary, PhD
Degree Date: August 2020

ABSTRACT

Bone mineral density (BMD), among other factors, largely effect the initial stability of the cementless tibial tray component in a total knee replacement (TKR), where increased motion at the tray-bone interface hinders bony ingrowth. With a lack of bony ingrowth, the cementless implant will not experience long-term success. Understanding which factors influence initial stability yields insight into surgical technique considerations and help inform a surgeon's implant choice. The objective of this study was to evaluate factors influencing the initial stability of cementless tibial trays using a 6-degree of freedom (6-DOF) robotic joint simulator, the AMTI VIVO, and combined loading scenarios replicating physiological loads experienced *in vivo* such as gait, stair descent and deep knee bending cycles. Prior to testing, cadaveric tibia were implanted with either cementless DePuy Attune RP, cementless DePuy Attune FB or cementless Stryker Triathlon FB and were impacted with either a traditional mallet or the Kincise, an automated surgical impaction device by a board certified orthopaedic surgeon. Medial, central and lateral markers were then placed on the anterior portion of the tibia and tibial tray to accurately measure displacements using a Digital Image Correlation (DIC) camera and software. Preoperative CT scans of the tibia were used to perform a virtual surgery on the specimen, and the segment of the tibial bone from the proximal cut to the distal tip of the tray's central cone were isolated. This tibial segment was meshed with 0.8-mm tetrahedral elements (Hypermesh, Altair, Troy, MI) and Hounsfield units for each element were extracted from the DICOM using custom Matlab

scripting and converted to bone mineral density using the known densities of the phantom. The ratio of tray coverage, the tibial plateau area of the tray within the peripheral border, was approximated and evaluated as a potential factor influencing initial stability. BMD was found to be a strong contributing factor to initial stability, especially for RP tibial trays. Conversely, tray coverage was not a strong contributing factor. The Kincise yielded positive results as compared to the mallet for tibia with high BMD values and tibia implanted with RP tibial trays. These findings assist in reforming surgical technique and help discern variables a surgeon should consider when selecting the optimal implant for a patient.

ACKNOWLEDGEMENTS

First and foremost, I must thank my advisor Dr. Chadd Clary for his continual guidance and mentorship. I am incredibly thankful for his support on this work and all the knowledge he has shared.

I want to thank Dr. Paul Rullkoetter and Amin Khodaei for serving as members of my defense committee.

I would like to thank Yashar Behnam for his time and assistance on numerous micromotion studies throughout the course of my degree. I also thank Mohsen Sharifi Renani for his assistance during micromotion studies and for his guidance with MATLAB script development for the micromotion study.

I would like to thank DePuy Synthes for their sponsorship of this study and for providing the necessary equipment throughout. In particular, I would like to thank Dr. Brian Haas.

Finally, I would like to thank all members of the DU Center of Orthopaedic Biomechanics. Their help and continued support both in the laboratory during surgeries and in the office are greatly appreciated.

TABLE OF CONTENTS

ABSTRACT ii

ACKNOWLEDGEMENTS iv

CHAPTER 1. INTRODUCTION 1
1.1 Introduction 1
1.2. Objectives 3
1.3 Thesis Overview 3

CHAPTER 2. BACKGROUND INFORMATION AND LITERATURE REVIEW 5
2.1 Cementless TKA 5
2.2: Mechanical Testing of the Initial Stability of Cementless Tibial Trays at the Tray-Bone Interface 7
2.3: Factors influencing the initial stability of implants 10
FIGURES AND TABLES 134

CHAPTER 3: EFFECTS ON INITIAL FIXATION OF CEMENTLESS TIBIAL TRAYS IN TOTAL KNEE ARTHROPLASTY 15
3.1 Introduction 15
3.2 Methods 17
3.4 Results 23
3.5 Discussion 28
FIGURES AND TABLES 34

CHAPTER 4: CONCLUSIONS AND RECOMMENDATIONS 52
4.1 Key Findings 52
4.2 Limitations and Future Work 53

BIBLIOGRAPHY 55

LIST OF FIGURES

FIGURE 2.1: TOTAL KNEE ARTHROPLASTY COMPONENTS.............................. 13
FIGURE 2.2: POROUS SURFACE OF DEPUY ATTUNE FEMURE IMPLANT........ 14
FIGURE 2.3: AMTI VIVO 6-DOF ROBOTIC JOINT SIMULATOR 14

FIGURE 3.1: THE FINITE ELEMENT LOWER LIMB MODEL USED TO CREATE IMPLANT SPECIFIC VIVO BOUNDARY CONDITIONS 36
FIGURE 3.2: KINCISE SURGICAL AUTOMATED SYSTEM 36
FIGURE 3.3: VIVO SIMULATOR LOADING IMPLANTED TIBIA. DIC RECORDING TRAY-BONE DISPLACEMENT FOR TARGETS APPLIED ON IMPLANT/BONE INTERFACE (INSET).. 37
FIG:URE 3.4: S-I, A-P, AD-AB, AND I-E LOADING PROFILES FOR GAIT, STAIR DESCENT AND DEEP-KNEE BENDING BASED ON ASTM F3141 AND SUPPLEMENTED WITH DATA EXTRACTED FROM THE ORTHOLOAD DATABASE 38
FIGURE 3.5 : DISTANCE BETWEEN TIBIAL MARKERS.. 40
FIG:URE 3.6: VIRTUAL SURGERY ON TIBIA 40
FIGURE 3.7: ANTERIOR BASEPLATE MOTION RELATIVE TO BONE FOR COHORT 1: KINCISE VERSUS MANUAL IMPACTION OF ATTUNE RP CEMENTLESS TIBIAL TRAYS... 41
FIGURE 3.8: ANTERIOR BASEPLATE MOTION RELATIVE TO BONE FOR COHORT 1: ANTERIOR BASEPLATE MOTION RELATIVE TO BONE FOR COHORT 2: KINCISE VERSUS MANUAL IMPACTION OF ATTUNE FB CEMENTLESS TIBIAL TRAYS... 42
FIGURE 3.9: ANTERIOR BASEPLATE MOTION RELATIVE TO BONE FOR COHORT 3: TRIATHLON VS ATTUNE FB CEMENTLESS TIBIAL TRAYS. 43
FIGURE 3.10: ANTERIOR BASEPLATE MOTION RELATIVE TO BONE FOR COHORT 1: COMPARISON OF ANTERIOR BASEPLATE MOTION RELATIVE TO BONE BETWEEN COHORTS FOR CENTRAL MARKER PAIRS 44
FIGURE 3.11: TOTAL DISTANCE VERSUS MAX-MIN DISTANCE FOR STAIR DESCENT, GAIT, AND DEEP-KNEE BENDING 44
FIGURE 3.12: AVERAGE TIBIAL MICROMOTION OF CLUSTERS BASED ON BMD AND TRAY COVERAGE. 45
FIGURE 3.13: SCATTER PLOT OF BMD VERSUS TRAY DISPLACEMENT DURING STAIR DESCENT BASED ON TRAY SIZE. 45
FIGURE 3.14: COMPARISON OF RP VERSUS FB ON AVERAGE TIBIAL MICROMOTION OF CLUSTERS BASED ON BMD AND TRAY COVERAGE. 46
FIGURE 3.15: SCATTER PLOT OF BMD VERSUS TRAY DISPLACEMENT DURING STAIR DESCENT SEPARATED BY IMPACTION METHOD.. 46
FIGURE 3.16: SCATTER PLOT OF BMD VERSUS TRAY DISPLACEMENT DURING STAIR DESCENT SEPARATED BY IMPACTION METHOD AND IMPLANT TYPE. 47
FIGURE 3.17: SCATTER PLOT OF BMD VERSUS TRAY DISPLACEMENT DURING STAIR DESCENT BASED ON GENDER 47

FIGURE 3.18: AVERAGE TIBIAL MICROMOTION AND BMD OF CLUSTERS GROUPED BY AGE 48
FIGURE 3.19: SCATTER PLOT OF TRAY DISPLACEMENTS VERSUS BMI 48
FIGURE 3.20: AVERAGE TIBIAL MICROMOTION OF CLUSTERS BASED ON BMI 49
FIGURE 3.21: SCATTER PLOT FOR COMPARISON OF BMI VERSUS BMD 49
FIGURE 3.22: TRAY DISPLACEMENT VERSUS BMD WITH INTRAOPERATIVE SURGEON CLASSIFICATION OF BONE QUALITY 50
FIGURE 3.23: BAR PLOT OF TRAY DISPLACEMENT FOR SURGEON CLASSIFICATION OF BONE QUALITY 51

CHAPTER 1. INTRODUCTION

1.1 Introduction

Annually, millions of orthopaedic medical devices are implanted in patients around the world for a multitude of reasons. The number of Total Knee Arthroplasties (TKA) has largely increased over the last several years due to osteoarthritis (OA) within the knee joint. The knee joint consists of the tibiae, femur, patella, tendons and several ligaments, providing stability to aid in proper joint function. When exhibiting OA, a patient experiences pain within the knee joint that will restrict their range of motion (ROM) and their ability to function normally. TKA aims to restore the patient's ROM without prolonged pain.

Cementless TKA implants have regained favor due to advancements in manufacturing and implant design (Crook et al., 2017). Currently, aseptic loosening is the lead cause of revision for TKA. Cementless implants can allow for greater osseous integrations resulting in long-term biological fixation, thus minimizing this cause of failure (Fricka et al., 2015). The main concern with cementless implants is the initial fixation of the tibial component. In order to ensure bony ingrowth and survivorship, the tibial component should not experience large displacements that would inhibit bony ingrowth (Chong et al., 2010). Evaluating the influence of factors such as bone mineral density (BMD) on tray-bone displacements under loads simulating activities of daily living is critical to understanding initial fixation of cementless tibial trays.

Previous studies quantified the effects of motion on bone ingrowth (Pillar et al., 1986, Bragdon et al., 1996, Jasty et al., 1997), while other *in vitro* studies focused on replicating loads experienced during activities of daily living (Baldwin et al., 2012, Clary et al., 2013). These mechanical testing rigs allow for cadaveric *in vitro* experimental studies focused on quantifying initial fixation of tibial implants that most closely resemble *in vivo* conditions with the advantage of controllable and repeatable physiological loading conditions. Additional studies focused on the relationship between BMD and implant fixation (Marquezan et al., 2012, Favre et al., 2016, Batz et al., 2019), but to our knowledge, none have focused on the correlation between BMD and initial stability of tibial implants specifically.

The primary objective of this thesis is to evaluate the influence of BMD and tray coverage on initial tibial fixation of cementless tibial implants during loading conditions simulating activities of daily living. Activities of daily living were replicated using a 6-degree of freedom (DOF) robotic joint motion simulator, the AMTI VIVO (AMTI, Watertown, MA). The micromotion at the anterior aspect of the tray-bone interface was evaluated for different implants and variations in tibial impaction method. These findings have significant clinical relevance regarding the influence of impaction method, BMD and tray coverage on initial fixation of cementless tibial trays and facilitate in selection of optimal candidates for cementless implants.

1.2. Objectives

The objectives of this thesis are to:

1. Compare and evaluate initial stability of several cementless tibial implants and impaction methods during simulated activities of daily living.
2. Provide verification for a finite element computational model of the experiment.
3. Evaluate the influence of BMD and tray coverage on initial tibial fixation of a cementless tibial implant after TKA.

1.3 Thesis Overview

Chapter 2 provides a brief background on cementless tibial implants, and a review of published literature on in vitro biomechanical testing and the effects of BMD on cementless tibial implants.

Chapter 3 presents *Effects on Initial Fixation of Cementless Tibial Trays in Total Knee Arthroplasty* that aims to characterize the effects of BMD and tray coverage on different implants on tray-bone micromotion during activities of daily living.

Chapter 4 discusses the significance of these findings and offers recommendations for future work.

CHAPTER 2. BACKGROUND INFORMATION AND LITERATURE REVIEW

2.1 Cementless TKA

TKA is a common and successful global orthopaedic procedure that has been performed millions of times. TKA aims to restore function of the knee and relieve the patient's pain, typically due to arthritis within the joint. TKA implant systems consist of metal-backed tibial and femoral components, a polyethylene patella component and a polyethylene spacer (Figure 2.1). TKA implants are often classified by two modes of fixation: cemented or cementless. Cemented fixation has been the favored mode of fixation by the majority of surgeons. Previous reports state cementless tibial implants have inferior long-term survival results compared to cemented (Illgen et al., 2004, Duffy et al., 1998). However, in recent years, cementless TKA implants have regained favor due to advancements in highly porous trabecular metallic surfaces (Figure 2.2). Aseptic loosening is the leading cause for revision of both cemented and cementless implants, and theoretically this increased porosity in cementless implants allows for greater osseous integrations resulting in long-term biological fixation, thus minimizing this cause of failure (Crook et al., 2017, Fricka et al., 2015).

Cementless fixation offers numerous potential benefits such as decreased operating time, preservation of bone stock, ease of revision and elimination of loose third body fragments (Fricka et al., 2015). Total knee replacements are projected to grow 85%, to 1.26 million procedures by 2030 (Sloan et al., 2018). Further, it is projected that 55% of TKA's in 2030 will be performed in patients younger than 65 years of age. This number can partially be attributed to a projected increase in obesity in future years (Kurtz et al., 2009). Younger, active and obese patients exhibit increased stresses on the bone-tray interface and have an increased likelihood for earlier loosening rates (Gustke, 2017). McCalden et al. found that 10-year survivorship was 98% in patients over 70 years of age, 96% in patients 56-65 years of age and 92% in patients younger than 55 years of age (McCalden et al., 2013). Similarly, Kerkhoffs et al. reported that obese patients required revision more often with an odds ratio of 1.30 (Kerkhoffs et al., 2012). With an increase in the prevalence of younger and obese patients, the need for cementless implants will rise. Cementless implants have the potential to utilize the biological fixation features by repairing and strengthening the bone-tray interface during these increased loading conditions. Because bony ingrowth plateaus around 9-months (Hofmann et al., 1997), a main concern with the cementless tibial implants is the initial stability prior to the bone ingrowth.

2.2: Mechanical Testing of the Initial Stability of Cementless Tibial Trays at the Tray-Bone Interface

In Vitro Testing

While *in vitro* experimental mechanical testing of cementless tibial implants cannot replicate bony ingrowth, the experiments are useful to evaluate an implant's initial stability by measuring the micromotion, the implant-bone movement. To correlate *in vitro* micromotion with bony ingrowth, *in vivo* studies quantifying effects of motion on bony ingrowth are needed. One canine *in vivo* study reported motions exceeding 150μm inhibited bony ingrowth (Pillar et al. 1986). Two additional canine studies reinforced these findings, reporting trabecular fractures for micromotion exceeding 150μm (Bragdon et al.; 1996, Jasty et al., 1997). Further, a greater amount of bone growth was associated with lower micromotions, most notably for motion less than 20μm. In addition to animal experiments, human *in vivo* experiments measure bone ingrowth for implanted cementless tibial trays in several ways. One method involves mapping and quantifying the bone ingrowth in retrieved cementless tibial trays. Baral et al. found that contemporary designs yield a mean bone ingrowth of 51.4%, as compared to previous designs with only 30% bone ingrowth (Baral et al., 2020). Alternatively, Russell et al. followed up with 72 cementless TKA patients over 2 years to review early clinical outcomes such as surgical time, estimated blood loss, Knee Society score pain, range of motion and radiographs (Cohen et al., 2018). The radiographs in this study were void of radiolucent and sclerotic lines, indications of loosening or migration, for 95% of patients. The remaining 5% exhibiting less than 1mm, nonprogressive radiolucent lines were further examined and not thought to represent loosening. These studies reinforce that improvements on contemporary cementless tibial implant designs result in increased survivorship due to successful bony ingrowth. To achieve greater success when designing new tibial trays, the initial stability must be less than 150μm to promote bony ingrowth.

In vitro testing is the preferred method to evaluate the initial stability of new tibial implant designs, where loads are applied to the knee joint while recording the implant micromotion and knee kinematics. *In vitro* experimental knee designs are most useful when micromotion is measured accurately without significant alterations to the tibia and when controllable and repeatable physiological loads are applied to the knee joint. Dynamic *in vitro* testing has many advantages over static *in vitro* testing as it can more effectively replicate *in vivo* post-operative conditions. Bhimji and Meneghini evaluated the effects of a compressive load compared to a loading profile simulating the stair descent activity, consisting of a combination of a compressive load, anterior-posterior load and an internal-external rotation, on tray-bone displacements. The study reported far greater magnitudes of tray-bone displacements for the multi-axial loading as compared to the single axial compressive load, demonstrating the importance of incorporating more complex loading conditions (Bhimji and Meneghini, 2012).

Multiple configurations of experimental knee simulators have been developed to compare and evaluate current and prospective knee implant designs. Testing rigs have progressed from mechanical testing machines measuring geometric constraints of implants experiencing compressive, cyclic anterior-posterior or internal-external loads (Haider and Walker, 2005) to simulators designed for six-degree-of-freedom (6-DOF) complex multi-axial physiological loadings at the knee such as the Kansas Knee

Simulator (Clary et al., 2013). The Kansas knee simulator and the Stanmore knee simulator, among others, utilize computational finite element models to replicate physical tests and have been validated with experimental data (Baldwin et al., 2012, Knight et al., 2007, Godest et al., 2002). The AMTI VIVO (Figure 2.3) (AMTI, Watertown, MA) allows for displacements or loads to be applied in any combination for the 6-DOF, making it one of the most sophisticated implant testing machines. The VIVO supports loads and kinematics in the Grood and Suntay coordinate systems (Grood and Suntay 1983), the biomechanic joint testing standard used by organizations such as ASTM, ISB and ISO.

Micromotion Measurement of Cementless Tibial Trays

Many *in vitro* biomechanical studies use human cadaveric tibiae or synthetic bone to replicate *in vivo* human bone. The material used to replicate *in vivo* human properties can significantly influence biomechanical experimental results (Basso et al., 2014). Sawbone (Sawbones, Pacific Research Laboratories, Inc., Vashon, WA) is one of the most commonly used synthetic bone consisting of fiberglass-reinforced epoxy and polyurethane foam to simulate cortical and cancellous bone. Sawbones are useful when evaluating various aspects of cementless implant designs due to its' repeatable placement and uniform material properties and consistent sizing (Bhimji and Meneghini, 2014, Crook et al., 2017), unlike cadaveric studies where cadavers present large variability in anthropometry and mechanical properties. Although cadaveric experiments are often more costly, human cadaveric tibiae provide results most closely resembling initial fixation conditions *in vivo* due to the incorporation of a surgeon and actual human tibial mechanical properties (Chong et al., 2017).

The method used to capture accurate micromotion between the implant and the bone is another important aspect in the experimental setup. The motion between cadaveric bone and an implant has been measured with inductive sensors (Bieger et al., 2013, Pal et al., 2010, Nadorf et al., 2014) and linear variable differential transducers (LVDTs) (Crook et al., 2017). In recent years, digital image correlation (DIC) has been used to measure implant-bone stability. DIC provides a non-contact stereo-camera system able to measure three-dimensional micromotion with greater precision than alternative methods such as LVDTs (Small et al., 2016). Yildirim et al. used a DIC GOM ARAMIS stereo-camera system (GOM mbh, Braunshweig, DE) to measure motions at the tibial-tray interface of uni-condylar knee replacements (UKR). The study reported the greatest motions were experienced on the anterior aspect of the tray-bone interface (Yildirim et al., 2016). This study demonstrates success of a DIC system as well as the importance of capturing motions at the anterior aspect of the interface.

2.3: Factors influencing the initial stability of implants

Bone Mineral Density

The relationship between bone mineral density (BMD) and implant fixation has been previously studied for hip stems and other implants, but very few studies have been conducted on the knee. Bone quality is an important criterion when selecting an implant for patients. Marquezan et al. found a positive correlation between BMD and initial stability of dental implants (Marquezan et al., 2012), and a separate study on osteoporotic vertebrae found a close correlation between BMD and pedicle screw stability (Weiser et al., 2017). Additionally, an *in vitro* shoulder experiment found agreeable results. The study implanted 18 stemless humeral implants into cadaveric humeri and measured implant micromotion under dynamic loading. Cancellous bone density had a significant effect on implant micromotion, resulting in the conclusion that only patients with adequate bone quality should be candidates for this procedure (Favre et al., 2016).

Further, patients with osteoporosis are more likely to experience periprosthetic fracture and require revision (Meek et al., 2011). When compared to cemented total hip replacements (THR), patients with good bone quality receiving THR often result in fewer complications (Gargiulo et al., 2013). Gender and age are often used as indicators of bone quality. Because bone quality typically declines with age, and women tend to exhibit decreased levels of bone quality as compared to men, older and/or female patients receive a greater number of cemented implants (Gargiulo et al., 2013, Magnusson et al., 2015). Petursson et al. explored the correlation between a patient's fracture risk index (FRI) and BMD, resulting in at least two out of ten patients who likely received nonideal implants. The study reported the highest BMD was found in a female who was the second oldest amongst the subjects; however due to the gender and age, she received a cemented stem. The study noted an inverse correlation between BMD and the percentage of fractured elements found using an FEA simulation, indicating BMD may be a useful measurement for a surgeon when discerning the optimal implant for a patient (Petursson et al., 2015). Batz et al. found that higher BMD led to improved densification around hip stems but also potentially prevented complete seating of the implant and that low-quality bone had a higher risk of fracture. While it is intuitive that higher quality bone would improve fixation, the interface mechanics of hip stems involve high shear loading while tibial trays are primarily loaded with compression and flexion moments which may change the effects of BMD (Batz et al., 2015). Gebert et al. investigated the effect of press-fit parameters on the primary stability of cementless femoral head resurfacing prosthesis. The FE model predicted increased stability with increased interference, bone quality and friction coefficient, but the experimental results did not agree. The variations between FE and experimental results may be due to the collapse of bone structures at increased interferences (Gebert et al., 2009).

When TKA is performed, aseptic loosening and poor outcomes increase with osteoporotic patients (Meet et al., 2011). Walsh et al. evaluated the role of stem extensions in osteoporotic tibia for TKAs and found statistically significant decreases in micromotion for cemented implants with stem extensions compared to primary implants with solely surface cement (Walsh et al., 2019). The results indicate that cemented primary implants alone do not provide sufficient stability for patients with poor bone quality. These studies indicate there is likely a relationship between bone mineral density and initial stability, but additional factors, such as the ability to fully seat an implant in sclerotic bone, may influence initial stability as well.

Understanding the contribution of each factor influencing the initial stability of cementless tibial implants may prove useful when designing cementless implants and when discerning the optimal implant for a patient. Future studies on initial stability should consider previous investigations and address any shortcomings. A critical takeaway from the literature reviewed is the need for studies evaluating the correlation between bone mineral density and the initial fixation of cementless tibial implants in order to better discern which candidates are best suited for cementless tibial implants. To investigate this, clinically relevant 6-DOF loading conditions for activities of daily living must be applied to cadaveric tibiae implanted with cementless tibial trays. Prior investigations indicate DIC is the more accurate and preferred method for recording micromotions. Unlike LVDTs which are unidirectional, DIC records measurements in three-dimensions and should be used to measure micromotions. Furthermore, the initial stability of different implant designs should also be investigated.

FIGURES AND TABLES

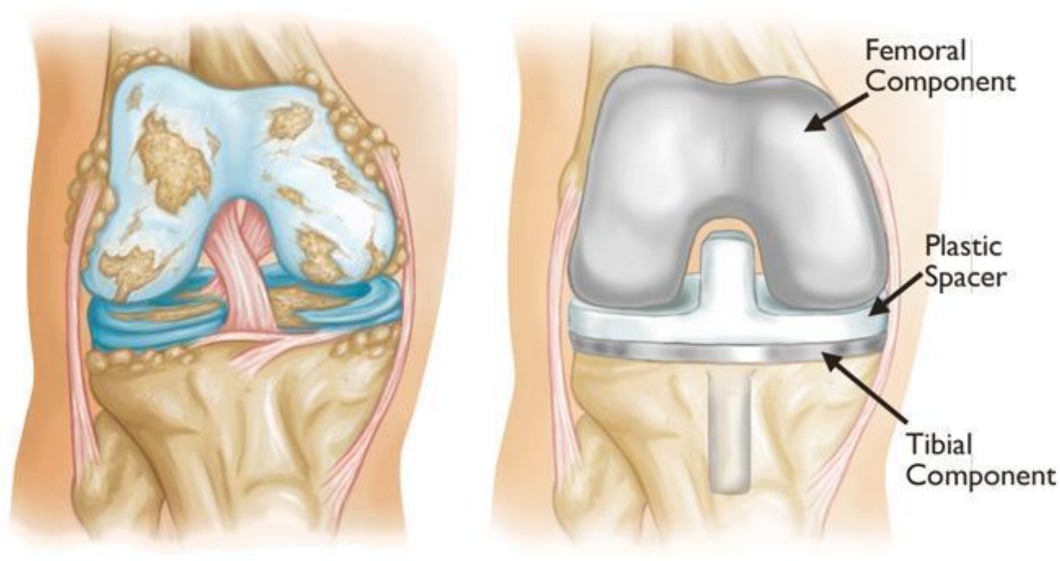

Figure 2.1 Total Knee Arthroplasty Components

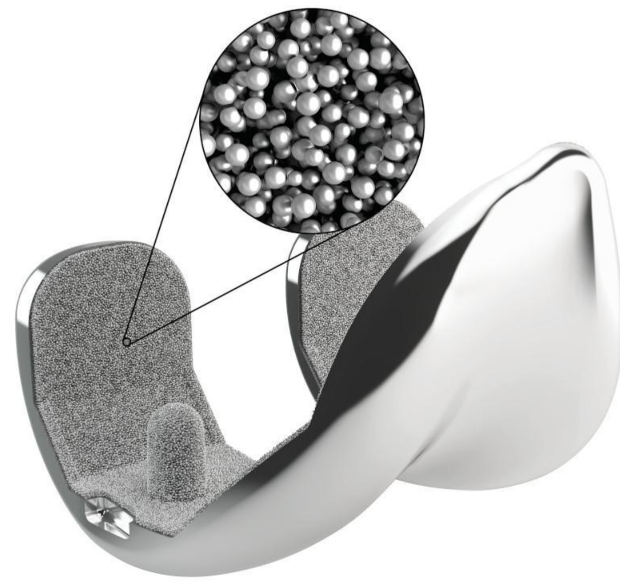

Figure 2.2 Porous Surface of DePuy Attune Femur Implant

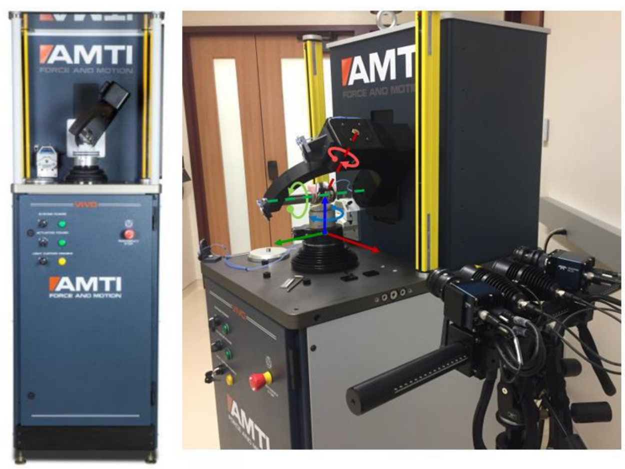

Figure 2.3 AMTI VIVO 6-Degree of Freedom Robotic Joint Simulator

CHAPTER 3: EFFECTS ON INITIAL FIXATION OF CEMENTLESS TIBIAL TRAYS IN TOTAL KNEE ARTHROPLASTY

3.1 Introduction

In recent years, cementless tibial implants have regained favor due to advancements in additive manufacturing and improvements in tibial tray designs. With successful long-term bony ingrowth, cementless TKA implants can withstand increased stresses placed on implants by active or obese patients, eliminate loose third-party fragments and result in more simplistic revisions (Gustke, 2017; Fricka et al., 2015). To obtain long-term bony ingrowth between the tibial implant and host bone, initial fixation of the implant is critical. *In vivo* canine studies found successful bone growth was associated with movements less than 20 µm and movements greater than 150 µm inhibited bony ingrowth (Pillar et al., 1986; Bragdon et al., 1996; Jasty et al., 1997). Initial fixation studies for TKA and total hip arthroplasty (THA) are often performed on cadavers by an orthopaedic surgeon to closely resemble *in vivo* conditions.

In vitro experimentation allows for invasive exploration of the knee joint but simulating *in vivo* physiological loading conditions is complex. Multiaxial dynamic loading conditions more accurately simulate *in vivo* conditions and result in increased magnitudes of tray-bone displacements as compared to single axial loading (Bhimji and Meneghini, 2012). The current top complex simulators utilize finite element models to replicate physical tests that have been validated with experimental data, such as the Kansas Knee Simulator and Stanmore Knee Simulator (Haider and Walker, 2005; Clary et al., 2013; Baldwin et al., 2012; Knight et al., 2007; Godest et al., 2002). These models are used to simulate activities of daily living to capture micromotion at the tray-bone interface that would closely resemble *in vivo* data. To further simulate *in vivo* data, a board-certified surgeon often performs the TKA on the cadaveric specimen.

Surgical factors often influence success of the TKA. One factor not yet explored in depth is the impaction method. Surgeons experience fatigue and work-related injuries due to repeated mallet use. To avoid this work-related injury, a surgeon would use an automated surgical system to replace the traditional mallet. The automated surgical system would deliver constant, consistent energy during impaction without the additional fatigue to the surgeon. The KINCISE (DePuy Synthes, Warsaw, Indiana), an automated surgical system used for total hip arthroplasties, is currently available for surgeons with favorable results, reducing operating room time by an average of eight minutes (Bhimani et al., 2019). One potential complication with the automated surgical system is the lack of feedback the surgeon experiences while impacting, which could result in the surgeon overimpacting the implant in soft bone. To quantify whether the automated surgical system is equivalent to impaction of a tibial implant with a mallet, an experimental study should focus on the influence impaction method has on micromotion of cementless tibial implants.

The primary focus of this study was to experimentally characterize the relationship between BMD, tray coverage and method of impaction with tray-bone displacements of cementless tibial trays *in vitro*. Micromotion was measured under loading conditions simulating activities of daily living such as gait, stair descent and deep knee bending. The BMD and tray coverage for each tibia were then analyzed, which have been shown to greatly impact initial stability of cementless implants (Favre et al., 2016; Marquezan et al., 2012; Batz et al., 2015). The work presented in this thesis has significant clinical relevance, given the projected increase in the need for cementless implants due to an increase in TKA patients that will likely exhibit greater stresses on the joint.

3.2 Methods

Initial Fixation Studies

Three cadaveric studies were conducted to evaluate the initial stability of cementless knee implants. The selection criteria for cadavers was no hardware in the knee or history of knee surgery, males (65”-70”) or Females (63”-66”), with a BMI less than 30 and age less than 80, although we deviated on height, age and BMI based on availability. Studies one and two evaluated whether differences in impaction devices influenced initial tray fixation, while study three quantified whether differences in implant design have a significant impact on initial tray fixation.

A previously validated finite element model of the lower limb was used to develop implant specific boundary conditions for the Attune cruciate retaining (CR) rotating platform (RP), Attune CR fixed bearing (FB), Attune posterior stabilizing (PS) FB, Triathlon CR FB, and Triathlon PS FB total knee replacement systems (Figure 3.1, Fitzpatrick et al., 2014). The external boundary conditions applied at the hip and ankle in the model were derived using the Orthoload database for gait, stair descent, and deep knee bending. The Attune RP (Size 5) and equivalent sizes of the Attune FB knee system (Size 5) and Triathlon FB knee system (Size 4) were virtually implanted into the model. In this way, the Attune and Triathlon implants were evaluated under a consistent set of boundary conditions while the resulting forces and moments applied to the tibial trays by the articulating surfaces were recorded and resolved about a point at the corresponding center of the RP or FB cone at the height of the proximal surface of the tibial tray. These resultant loading and kinematics were turned into implant specific loading profiles using MATLAB. The loading profiles were then loaded into the AMTI VIVO simulator and used in the subsequent mechanical testing to apply loads and moments for specific activities of daily living (Table 1).

Forty pelvis-to-toe tip specimen were acquired for the experiment. All trays were implanted by a fellowship trained orthpaedic surgeon. The specimen were implant with either an Attune Cementless RP tibial tray, Attune Cementless FB tibial trays or Triathlon Cementless FB tibial tray, as described by the following cohorts:

- Cohort 1: Mallet v. Kincise. 19 pelvis-to-toe tip specimen with 38 tibiae implanted with Attune Cementless RP.

- Cohort 2: Mallet v. Kincise. 13 pelvis-to-toe tip specimen with 26 tibiae implanted with Attune Cementless FB.
- Cohort 3: Attune Cementless FB v. Triathlon Cementless FB. 8 pelvis-to-toe tip specimen with 8 tibiae implanted with Attune Cementless FB and 8 tibiae implanted with Triathlon Cementless FB.

Cohort 1 and Cohort 2 evaluated impaction method. Trays were implanted using a mallet on the control side and Kincise on the contralateral side (Figure 3.2). Cohort 3 compared the micromotion of two cementless FB tibial implants by implanting Attune Cementless FB on one side and Triathlon Cementless FB on the contralateral side.

The surgeries were performed using the implant's recommended surgical technique. Specifically, for Attune implants, the tibiae were cut with 5°-7° of tibial posterior slope. After surgery, the implanted tibiae were extracted from the specimen, skeletonized, sectioned 125-mm below the joint line, and cemented into fixtures. DIC targets were applied along the anterior aspect of the tibial tray and along the anterior rim of the tibial cortex directly inferior to the cut plane. The central target was placed using the vertical line marked on the tibial tray implant, while the medial and lateral markers were placed on the outermost inscription on the tibial tray implant (Figure 3.3). The corresponding markers were then placed on the tibia. Three target pairs were identified, the central, the most medial and the most lateral pairs. Relative displacements between the pairs of targets were recorded using a GOM Aramis DIC system.

Each specimen underwent a series of standardized loading conditions in the AMTI VIVO, including the Triathlon specific boundary conditions for gait, stair descent, and deep knee bending (Figure 3.4, Table 1). Due to the low conformity of the Triathlon design, some of the loading profiles would only run on new inserts and would deform the posterior aspect of the insert over time leading to posterior dislocation (Orthoload Adduction Gait, Orthoload Adduction Stair Descent, Orthoload 75% Posterior DKB, Attune CR 50%, 75%, and 100% DKBs) . These dislocations were not observed on Attune. To prevent the dislocations, the loading profiles leading to dislocation were performed on new Triathlon inserts while the AP translation and IE rotations were recorded. These kinematics were then substituted as displacement inputs for the corresponding Triathlon boundary conditions for the actual testing. Forty cycles of each loading condition were applied while tibial tray/bone displacements were recorded on cycles 30-40. The maximum and minimum relative distance between each pair of DIC targets across the anterior aspect of the tibia was calculated, then the total change in distance was calculated as the maximum distance minus the minimum distance for each marker pair. The total change in distance was averaged across all specimen receiving the same implant type. Paired t-tests were performed to detect statistically significant differences between cohorts for each activity ($p < 0.05$). This procedure was replicated for each experiment within the three cohorts. Actuator displacements in the VIVO were used to calculate Grood and Suntay kinematics and compared between different implant designs.

Multiple methods exist in the literature for calculating micromotion. It is unclear if the methods impact whether there is a correlation within the data. The current method used for calculating the tray-bone displacements, the maximum distance minus the minimum distance, was compared to calculating tray-bone displacement as the total distance traveled (Figure 3.5). The total distance traveled was calculated by summing the distance using the following formula: $d = \sqrt{(x^2 - x^1)^2 + (y^2 - y^1)^2 + (z^2 - z^1)^2}$. A linear regression was performed to evaluate whether there was a linear correlation between the two methods.

Factors Effecting Initial Stability

BMD and ratio of tray coverage were explored to determine their contribution to the initial stability of the tibial tray. To quantify BMD, pre-operative CT scans were performed, incorporating a BMD phantom (Mindways, Austin, TX) placed beneath the knees, on the forty matched pairs of cadaveric human tibiae (80 total knees) tested in the initial fixation studies. Solid models of the tibia were segmented using ScanIP (Synopsis, Mountain View, CA). The tibiae were aligned anatomically using the origin, medial condyle, lateral condyle and ankle center. A virtual surgery was performed on the specimen, and the segment of the tibial bone from the proximal cut to the distal tip of the tray's central cone were isolated (Figure 3.6). This tibial segment was meshed with 0.8-mm tetrahedral elements (Hypermesh, Altair, Troy, MI) and Hounsfield units for each element were extracted from the DICOM using custom Matlab scripting and converted to bone mineral density using the known densities of the phantom. Elements containing cortical bone were excluded (BMD > than 600 kg/m^3) and the average BMD by volume was calculated for the remaining cancellous bone elements. During experiments, the surgeons were asked to state the specimen bone quality as either poor, fair, good or excellent. A t-test was performed to note any statistical significances between micromotion of intraoperative bone quality groups. Additionally, a linear regression was performed on the data to find any correlation due to gender or age.

The assumptions that were made when calculating the BMD were evaluated to ensure they do not greatly influence results. The surgical cut was not measured, therefore surgical parameters such as the resection were assumed when performing the virtual surgery. A sensitivity analysis was performed to quantify the amount of error introduced when assuming a 9mm cut depth. To do so, the sensitivity of cut depth was determined as the percent difference of BMD found by varying cut depth from 7 mm to 11 mm. Further, the threshold used to exclude cortical bone was assumed to be 600 kg/m^3. To evaluate this assumption, the percent difference of BMD was calculated by varying threshold values to exclude the cortical bone from 550 kg/m^3 to 650 kg/m^3.

Tray coverage was determined as the ratio of the area of tray within border of tibial plateau area for an approximation of coverage. Tray coverage was selected as a potential factor to influence initial stability because if the implant is largely undersized or overhang is evident, the tibia may experience increased stresses at undesirable points. To approximate tray coverage, assumptions were made for the surgical resection, including 0 degree varus-valgus slope, 5 degrees posterior slope and a cut depth of 9mm. Because these values were not measured, a sensitivity analysis of tray coverage was performed to ensure variability of these do not largely affect results. This was done by finding the standard deviation for each specimen when varying varus-valgus slope from -3 to +3 degrees, posterior slope 3 to 7 degrees, and cut depth 8 to 12mm. The mean of the standard deviation of all specimen was used to represent the confidence interval.

Tray-bone displacements for each tibia were clustered based on BMD into high (BMD>180 kg/m^3) and low (BMD<180kg/m^3) BMD groups, and tray coverage into high (coverage>0.86) and low (coverage<0.86) coverage groups. T-tests were performed to determine significant differences in micromotions between the groups.

The influence of additional variables on tray-bone displacements was examined. The data was further separated into two groups based on tray sizes. The first group consisted of large trays (size 6-8) and the second of small trays (size 4-5). A t-test was performed to determine statistical differences in micromotion between the two groups. Surgeons often assume bone quality based on a patient's gender or age, which can influence their decision when selecting the type of implant. Because of this, the influence of gender and age were explored by clustering the data based into groups (65 and younger/65 and older). Additionally, BMI was evaluated as a potential influence on tray-bone displacement. Tibias were clustered into low (BMI less than 24) and high (BMI 24 and greater) BMI groups, and tray displacements of the two groups were compared. A specimen's BMI and BMD were compared to note any visible trend in the data that would indicate whether BMI is unique to tray-displacements, regardless of BMD.

3.4 Results

Initial Fixation Results

Of the nineteen specimen in Cohort 1, twenty-nine tibiae ran successfully (Table 2 lists the outcome for each tibia within each cohort). Within Cohort 1, the trays impacted with the Kincise consistently demonstrated larger displacements compared to those impacted with the mallet in stair descent and gait. The greatest tray displacements were recorded during gait and stair descent activities (Figure 3.7). Statistically significant ($p < 0.05$) increases in tray displacements were observed on the all aspects of the tray for the deep-knee bending neutral activity (Table 3). Stair descent neutral and gait neutral activities were trending toward statistical significance ($0.09 < P < 0.15$) for the medial and central aspects of the tray.

Within Cohort 2, seventeen of the twenty-six tibiae tested ran successfully. Tibiae within this cohort exhibited larger tray-bone displacements during stair descent neutral and gait neutral as compared to the relatively low motions experienced during deep knee bend neutral (Figure 3.8). There were no statistically significant differences between tibiae impacted with the Kincise and tibiae impacted with a mallet. The central marker experienced the greatest micromotion for each activity, regardless of impaction method.

The five remaining successful matched pairs in Cohort 3 yielded full data sets for all loading conditions. The biggest tray displacements were observed during Gait Triathlon CR, Stair Descent Attune CR, Stair Descent Triathlon CR, and DKB Anterior CR. In three specimen, the Triathlon implanted tibiae showed markedly higher micromotions than the corresponding Attune implanted tibia (one of these specimen with observed subsidence of the Triathlon implant). In the remaining three specimen, the micromotion between Attune and Triathlon were equivalent. When tray-bone displacements were averaged across specimen, no statistically significant differences were observed (Figure 3.9, $P < 0.05$). However, tray-bone displacement differences observed on the lateral aspect during stair descent neutral and deep knee bend activity and medial aspect during stair descent were approaching statistical significance ($0.09 < P < 0.15$. Table 3).

When all three cohorts were compared, Cohort 1, containing Attune RP Cementless implants, exhibited the largest micromotion for stair descent neutral, gait neutral, and deep knee bending neutral as compared to the other two cohorts (Figure 3.10). The means for stair descent neutral and gait neutral within Cohort 2, containing FB Attune Cementless, were greater than Cohort 3, containing Attune FB versus Triathlon FB.

The method for calculating micromotion was explored for data within all cohorts. For the max-min method, the largest displacements were associated with the central marker, while the total distance method had the largest displacements associated with both the medial and lateral markers. The results using each method were then compared using a linear correlation (Figure 3.11). There is not a strong correlation, indicating that although averaged results were greatest using both methods for similar activities, individual results may contain outliers. The strongest correlation between the two methods was seen for stair descent, followed by gait, followed by DKB.

Results of Factors Effecting Initial Stability

Of the 80 knees tested in the protocol, 57 withstood the loading with no signs of loosening, while five bones failed with subsidence of the tray and the remaining seventeen bones fractured. Average cancellous BMD for the specimen ranged from 60.4 to 267 kg/m^3 with a mean of 157.5 kg/m^3 and a median of 159.5 kg/m^3. The mean BMD for the specimens that failed ranged from 60.4 to 169.6 kg/m^3. Largest tray-bone displacements were consistently observed during stair descent and gait, followed by deep knee bending. Based on a clustering analysis, statistical significance differences were noted between BMD and tray displacements during stair descent, gait, and deep-knee bending activities (Figure 3.12). There were statistical significant differences for all stair descent, gait, and deep-knee bending activities ($p = 0$, $p=0.002$, $p=0$, respectively) in micromotion between the low and high BMD groups. The mean tray coverage for the specimen was 0.82 and a median of 0.82. No statistically significant differences in micromotion were seen between low and high tray coverage clusters during the three activities ($p=0.7917$, $p=0.9309$, $p=0.7739$). Additionally, there is not a correlation between large and small trays for tray-bone displacements and BMD (Figure 3.13).

The results were further separated by FB and RP. The high and low BMD groups for Attune RP implants exhibited greater differences in tray-bone displacements as compared to Attune FB implants, most notably for the gait cycle (Figure 3.14). There were no statistical significances between the high and low BMD groups for the FB implants ($p =0.3212$, $p=0.2929$, $p=02711$, for stair descent, gait and deep knee bending, respectively). For the RP implants, only the gait cycle resulted in statistical significance between the groups ($p=0.0997$, 0.0115, 0.0815, for stair descent, gait and deep knee bending, respectively).

Within the dataset, 25 matched pairs of tibiae were tested in an impaction study. Of these tibia, tray-bone displacements and BMD were more linearly related for tibial trays impacted with the Kincise ($R^2=0.848$) as compared to trays impacted with a mallet ($R^2=0.024$), shown in Figure 3.15. Further, the impaction data was separated by implant type. The RP implant demonstrated a more linear correlation for the Kincise data as compared to the FB data (Figure 3.16).

Within the complete dataset, the BMD values were separated by gender, 38 male tibia and 24 female tibiae (Figure 3.17). Of these tibia, 12 male tibiae failed (31.6%), and 5 female tibiae failed (20.8%) The average male and female BMD were 165.6 kg/m^3 and 161 kg/m^3, respectively. There was not a correlation between genders for BMD and micromotion, and statistical differences were not significant for stair descent, gait nor deep-knee bends between genders. Age was evaluated as a potential factor for influencing tray-bone displacements. The ages of the specimen ranged from 53 to 88 with a mean age of 73. Although the mean BMD and mean tray-bone displacements were greater for the 65 and older group, there were no statistical significances between the two groups (Figure 3.18). When considering the influence of a specimen's BMI, there was not a linear correlation between tray displacement and BMI ($R^2 = 0.16$). Further, there was a statistical significance between the low and high BMI groups, indicating BMI may be a contributing factor to initial stability of cementless tibial trays ($P = 0.0024$, Figures 3.19 and 3.20). Specimen had varying values of BMD for similar BMI, indicating the correlation between tray displacements and BMI are unique to BMI and likely not due to a patient's BMD (Figure 21).

Another way the tibiae were grouped was by the surgeon's classification of bone quality. All but two tibiae deemed poor bone quality failed, and no tibiae classified as either good or excellent bone quality failed. The two tibiae noted as poor quality that did not fail exhibited increased micromotion consistent with micromotion values of several other tibiae with similar BMD values. Overall, tray-displacement increased with a decrease in bone quality (Figures 3.22 and 3.23). When BMD was compared to surgeon bone quality, BMD increased as surgeon bone quality increased. BMD values for poor and fair bone were similar (BMD of 117.1 kg/m^3 and 128.4 kg/m^3, respectively).

Varying the threshold used to exclude cortical bone resulted in a maximum percent of BMD of 3.9% with a cut-off value of 650 kg/m^3. The range of percent differences of BMD with the 550 kg/m^3 and 650 kg/m^3 cut-off value were from 1.2 to 3.9 %. Similarly, the increased percent differences were seen in tibia with high BMD values. When the cut depth of the tibia was varied between 3mm less and 3mm greater, the maximum percent difference of BMD was 9.72% for a size 5 specimen with poor bone quality, whereas a maximum percent difference of BMD for a size 8 specimen with good bone quality was 4.24%.

The sensitivity analysis on ratio of tray coverage yielded a range between 0.689 and 0.982 and a standard deviation of 0.0064 for ratio of coverage between a cut depth of 8mm to 12mm. The smaller tibiae were more sensitive to an increased cut depth. Alternatively, posterior slope did not greatly alter tray coverage, with a range of 0.69 to 0.97 and average standard deviation of 0.0027 for ratio of tray coverage. Both increasing and decreasing the Varus-Valgus slope resulted in a range of 0.68 to 0.98 and an average standard deviation of 0.01 for ratio of tray coverage.

3.5 Discussion

Cementless TKA success can be heavily influenced by factors effecting the implant's initial stability. This study reports the effect of BMD and tray coverage on the tibial baseplate initial fixation of 80 specimen implanted with cementless tibial trays. In addition, it also quantifies whether differences in impaction devices and implant design have an impact on initial tray fixation and examines output kinematics of various cementless tibial trays. To our knowledge, no published literature exists regarding the influence of BMD on initial fixation of cementless tibial trays. This study is the first to investigate the effect of BMD to further understand the failure mechanism of aseptic tibial loosening conditions.

Initial Fixation of Cementless Tibial Trays

Tray displacement across the anterior aspect of cementless Attune FB, cementless Attune RP and cementless Triathlon FB tibial trays were evaluated under different activities of daily living, including gait, stair descent and deep knee bending. In general, the resultant micromotions at the tray-bone interface were consistent for each activity, with highest tray displacements occurring during stair descent activities. Additionally, resulting implant kinematics were consistent for each implant design.

Micromotions across the anterior aspect of the 19 successful specimen implanted with Attune RP implant system impacted with a mallet or Kincise device were evaluated under various activities of daily living, including gait, stair descent, and deep knee bending. The results demonstrated that the implant micromotion relative to the bone is sensitive to impaction method, especially for deep knee bending. In all specimen which were successfully tested, those impacted with the Kincise demonstrated higher micromotions under most gait cycles and several stair descent conditions. Kincise had favorable results for deep-knee bend but mallet was favorable for stair descent and gait.

Conversely, the 13 specimen implanted with Attune Cementless FB implant system demonstrated that the implant micromotion relative to the bone was not sensitive to impaction method. In some specimen, the side impacted by the mallet had higher micromotions, while the inverse was true for other specimen. When compared to Cementleess Attune RP, Cementless Attune FB had lower micromotion for all activities, indicating the fixation features of the Cementless Attune RP are not as robust as the Cementless Attune FB.

The micromotion comparison of initial fixation between the Triathlon and Attune FB cementless tibial trays indicate that implant micromotions between Triathlon and

Attune are not statistically significantly different, although some loading cases are trending toward a statistically significant reduction with Attune. The findings suggest that both the cementless Triathlon and Attune result in greater micromotion on the center and lateral side of the tibia, and both implants displayed small motion, most means less than 100 µm as compared to cementless Attune RP tibial trays with means near 150 µm. One limitation of the study was the limited number of successfully tested specimen (5 matched pairs) and could be improved through testing of additional specimen. Attune FB impacted with a mallet within Cohort 2 exhibited almost twice the level of micromotion for some activities as compared to Attune FB in Cohort 3. The discrepancy between the two is likely due to other factors more influential to the implant's initial stability.

When comparing the method for calculating micromotion, there is not a strong correlation between the two methods. Gaping between the implant and tibia largely inhibits bone growth. The max-min method is more sensitive to gaping, indicating it is a better method for calculating the micromotion that is harmful to bony ingrowth. The total distance method will better capture shear motion; however, this is not the main concern for interference with bony ingrowth. This shear motion captured in the total distance method likely contributes to the outliers, reducing the correlation between the methods. Future studies can evaluate using the total distance in the superior-inferior direction as a better representation of micromotion that is inhibitive of bony ingrowth.

Factors Effecting Initial Stability

BMD was a strong contributing factor to initial stability of cementless tibial trays for stair descent, gait and deep knee bending. The data suggests that a cancellous BMD threshold exists (<180 kg/m3), below which there is a high likelihood of increased micromotion, tray subsidence, and tibial fracture. Surgeons should implant cementless tibial trays in patients with good bone quality. If cementless implants are implanted in patients with low bone quality, the large tray-bone displacements would be deleterious to implant fixation.

Surgeons often decide whether to use a cementless implant on a patient based on the patient's gender or age. In the cadaveric study, 39 male tibiae and 24 female tibiae were used to discern whether there was a correlation between gender and tray-bone displacement. The results indicate average BMD was within 4 kg/m^3 between genders with a difference of 24 µm in average micromotion. Although there were not notable differences between genders, the greatest BMD was seen in a female specimen, indicating gender may not always be a good indicator of bone quality. Additionally, specimen younger than 65 had lower levels of micromotion, while greatest micromotion occurred with patients near 75 years of age. A patient's BMI was likely an additional contributing factor to increased tray displacements. Specimen with higher BMI values exhibited lower levels of micromotion, indicating BMI should be evaluated when considering cementless tibial implants. Because the number of younger and obese patients receiving TKA is projected to increase within the next few years, these results reaffirm that younger and obese patients may be good candidates for cementless implants seeing as the low levels of micromotion will allow for bony ingrowth. The cementless implants will allow for greater long-term fixation that will likely withstand greater loads, often exhibited by younger, active persons.

When comparing the influence of BMD on initial fixation based on Attune implant type, there was a stronger correlation for the high and low BMD groups for

Attune RP implants as compared to Attune FB implants, most notably for the gait cycle. Surgeons should use FB tibial implants for patients with lower BMD to provide the additional stability that will result in decreased tray-bone displacements to allow bony ingrowth. RP implants should instead be implanted in active patients with high BMD, where micromotion resides below the 150 µm.

Based on the impaction studies, the tibia impacted with Kincise exhibited a more linear correlation between micromotion and BMD as compared to those impacted with a mallet. The impaction study results were further separated by implant type with implants impacted with Kincise exhibiting greater tray-bone displacements for both FB and RP implants. The Kincise likely is better able to seat tibial trays in hard, sclerotic bone. Intraoperatively with sclerotic bone, surgeons can choose to drill small holes into the bone to aid in impaction of the implant. The Kincise can eliminate this additional step and decrease operating time for these patients. While using the Kincise, a surgeon exhibits less wear on their shoulder, thus retaining the ability to operate for a greater number of years. Alternatively, tibia with poorer bone quality impacted with Kincise exhibited larger micromotions as compared to bone impacted with a mallet. This is likely due to the lack of feedback for the surgeon during the impaction, which may cause damage to the tibia.

Intraoperatively, surgeons can discern bone quality relatively well. During the cadaveric studies, no tibia deemed good or excellent bone quality by the surgeons failed and all but two tibia deemed poor bone quality failed. The tibia deemed fair or poor by the surgeons are almost exclusively below the 180 kg/m^3 threshold. This has clinical relevance, because surgeons could decide intraoperatively whether to use a cementless implant on a patient by assessing the patient's bone quality. Calculating a patient's BMD preoperatively would be a better prediction of a patient's likelihood for successful bony ingrowth instead of using a surgeon's classification of bone quality intraoperatively. Several tibiae classified as good bone exhibited micromotion above 150 μm, indicative of inhibiting bony ingrowth. All of these tibiae had a BMD less than 180 kg/m^3, meaning BMD is a more reliable method for discerning the bone quality.

Tray coverage was not a strong contributing factor to the initial fixation of the tibial tray for neither stair descent, gait nor deep knee bending. There were no notable differences of mean micromotion values between coverage groups for either activity. The range of tray-bone displacement during the stair descent and gait activities were larger for the low coverage group as compared to the high coverage group. This could be an indication that tibia with low tray coverage could experience greater micromotion; however, tray coverage should not be the focus when designing cementless tibial trays for improved initial fixation.

FIGURES AND TABLES

Table 3.1: Activities with Abbreviations Applied to Specimen *(Disp.=Displacement control)*

Activity	Variation	Naming Convention	Triathlon Control Mode AP	Triathlon Control Mode IE	Attune Control Mode AP	Attune Control Mode IE
Gait Cycles	Orthoload - Neutral	GTON	Load	Load	Load	Load
	Orthoload - Adduction	GTOAD	Disp	Disp	Load	Load
	Attune CR Specific	GTATTCR	Load	Load	Load	Load
	Triathlon Specific	GTTRICR	Load	Load	Load	Load
	Orthoload - Neutral (PS)	GTONPS	Load	Load	Load	Load
Stair Descent Cycles	Orthoload - Neutral	SDON	Load	Load	Load	Load
	Orthoload - Adduction	SDOAD	Disp	Disp	Load	Load
	Attune CR Specific	SDATTCR	Load	Load	Load	Load
	Triathlon Specific	SDTRICR	Load	Load	Load	Load
	Orthoload - Neutral (PS)	SDONPS	Load	Load	Load	Load
Deep Knee Bending Cycles	Orthoload - Neutral (CR)	DKBON	Load	Load	Load	Load
	Orthooload - Anterior	DKBOAN	Load	Load	Load	Load
	Orthoload - 75% Posterior	DKBOPO75	Disp	Disp	Load	Load
	Attune CS Specific	DKBATTCS	Load	Load	Load	Load
	Attune CR Specific	DKBATTCR	Disp	Disp	Load	Load
	Attune CR Specific - 50% Posterior	DKBATTCR50	Disp	Disp	Load	Load
	Attune CR Specific - 75% Posterior	DKBATTCR75	Disp	Disp	Load	Load
	Orthoload - Neutral (PS)	DKBONPS	Load	Load	Load	Load
	Triathlon Specific	DKBTRI	Load	Load	Load	Load

Table 3.2: Outcomes for tibia in Cohort 1, Cohort 2 and Cohort 3

Cohort	Implant Type(s)	Variable	Number of Tibia Tested	Number of Successful Tibia	Number of Failed Tibia
Cohort 1	Cementless Attune RP	Impaction method	38	29	9
Cohort 2	Cementless Attune FB	Impaction method	26	19	7
Cohort 3	Cementless Attune FB and Cementless Triathlon FB	Implant Type	16	9	7

Table 3.3: P-values indicating statistically significant differences in tray displacements for all Cohorts for all Cohorts

Cohort	Activity	P-value		
		Medial	Central	Lateral
Cohort 1	Stair Descent Neutral	0.092	0.068	0.694
	Gait Neutral	0.092	0.890	0.543
	DKB Neutral	0.021	0.011	0.050
Cohort 2	Stair Descent Neutral	0.529	0.947	0.549
	Gait Neutral	0.247	0.487	0.867
	DKB Neutral	0.660	0.994	0.253
Cohort 3	Stair Descent Neutral	0.133	0.201	0.128
	Gait Neutral	0.545	0.556	0.458
	DKB Neutral	0.625	0.858	0.997

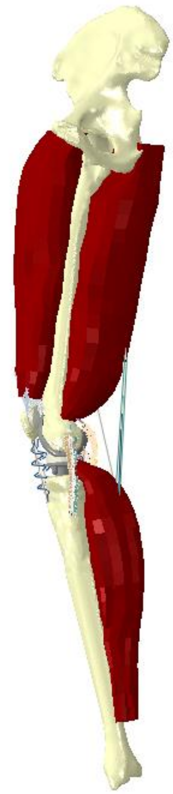

Figure 3.1 The finite element lower limb model used to create implant specific VIVO boundary conditions

Figure 3.2 Kincise surgical automated system

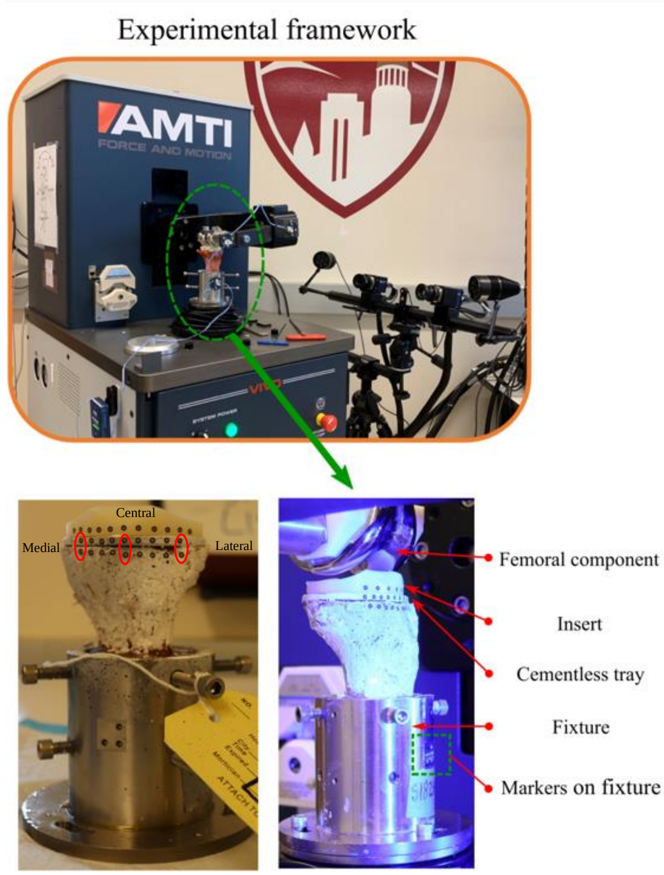

Figure 3.3 VIVO simulator loading implanted tibia. DIC recording tray-bone displacement for targets applied on implant/bone interface (inset)

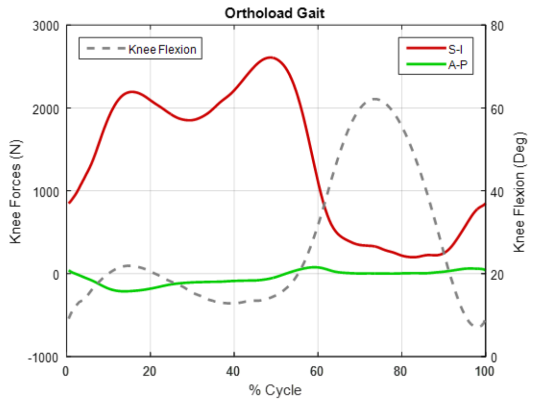
Orthoload Gait
Knee Flexion
S-I
A-P
Knee Forces (N)
Knee Flexion (Deg)
% Cycle

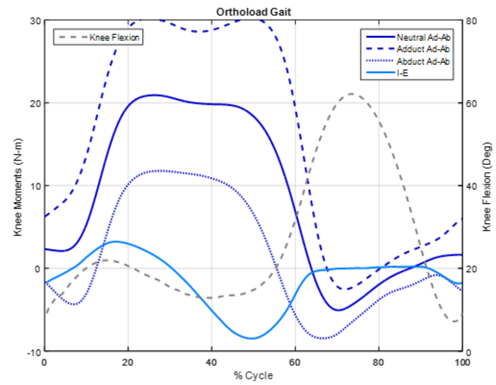
Orthoload Gait
Knee Flexion
Neutral Ad-Ab
Adduct Ad-Ab
Abduct Ad-Ab
I-E
Knee Moments (N-m)
Knee Flexion (Deg)
% Cycle

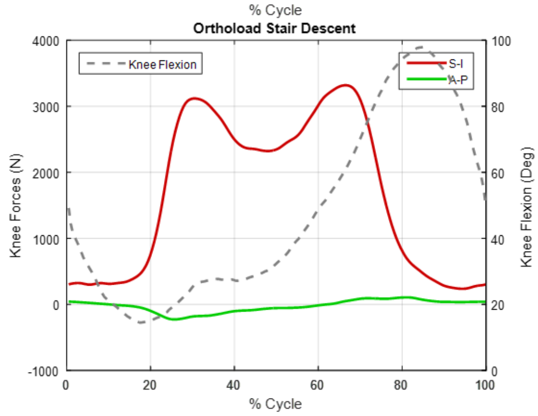
Orthoload Stair Descent
Knee Flexion
S-I
A-P
Knee Forces (N)
Knee Flexion (Deg)
% Cycle

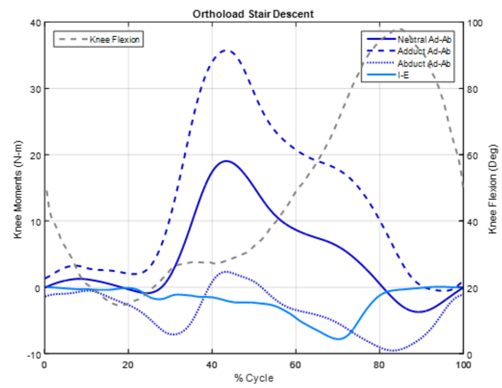
Orthoload Stair Descent
Knee Flexion
Neutral Ad-Ab
Adduct Ad-Ab
Abduct Ad-Ab
I-E
Knee Moments (N-m)
Knee Flexion (Deg)
% Cycle

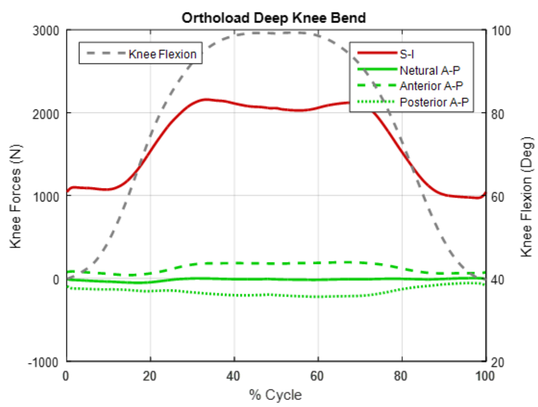
Orthoload Deep Knee Bend
Knee Flexion
S-I
Netural A-P
Anterior A-P
Posterior A-P
Knee Forces (N)
Knee Flexion (Deg)
% Cycle

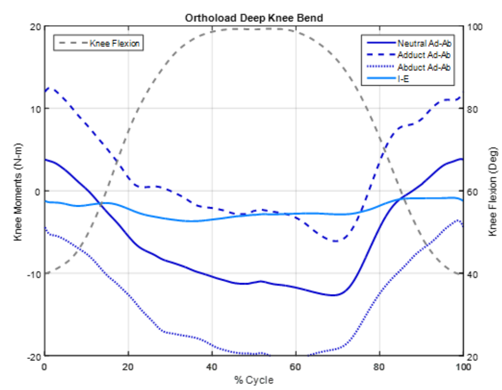
Orthoload Deep Knee Bend
Knee Flexion
Neutral Ad-Ab
Adduct Ad-Ab
Abduct Ad-Ab
I-E
Knee Moments (N-m)
Knee Flexion (Deg)
% Cycle

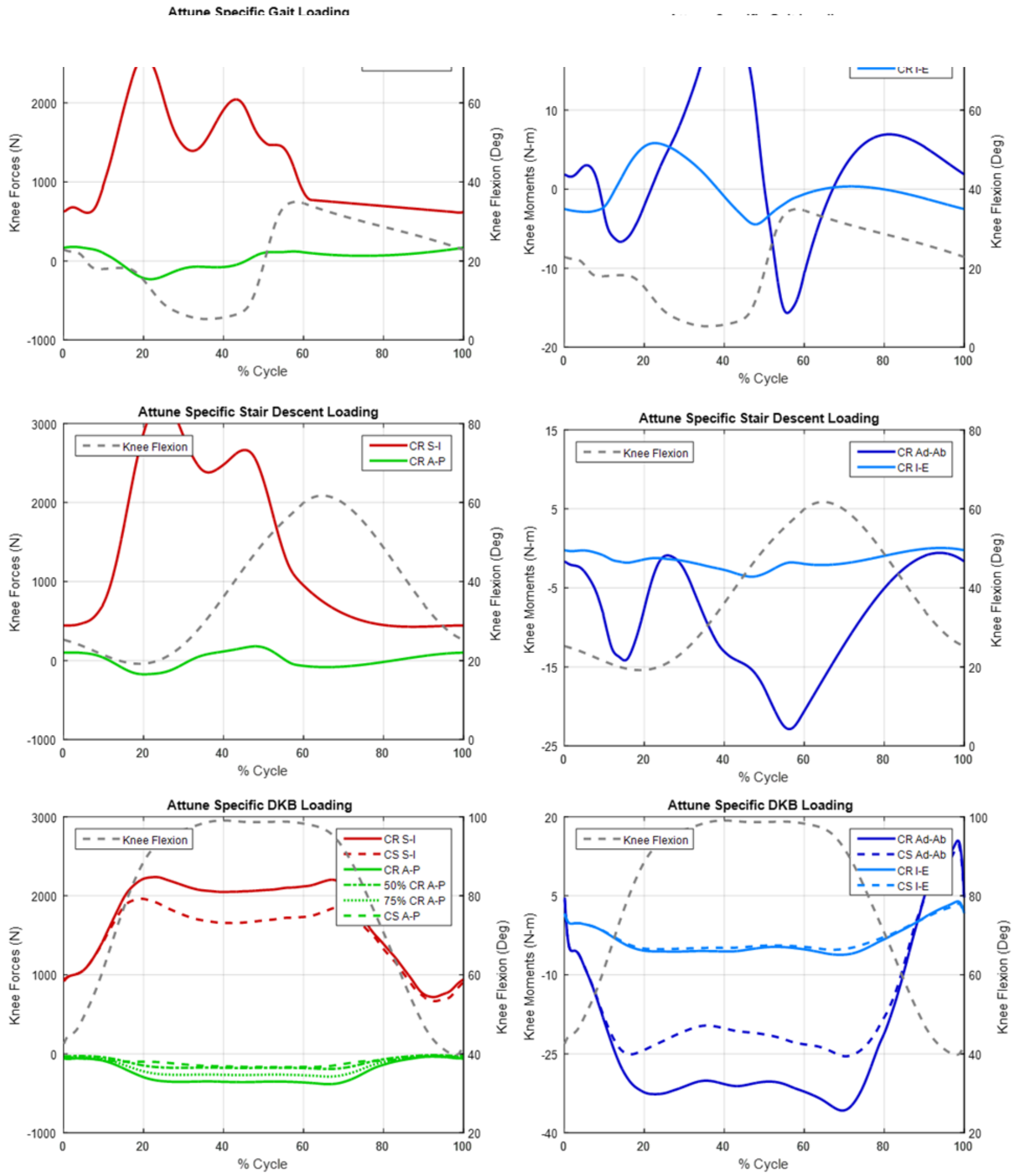

Figure 3.4: S-I, Ad-Ab, and I-E loading profiles for Gait (top), Stair Descent (middle), and Deep Knee Bend (bottom) based on Attune Specific loading conditions derived from computational models of the lower limb.

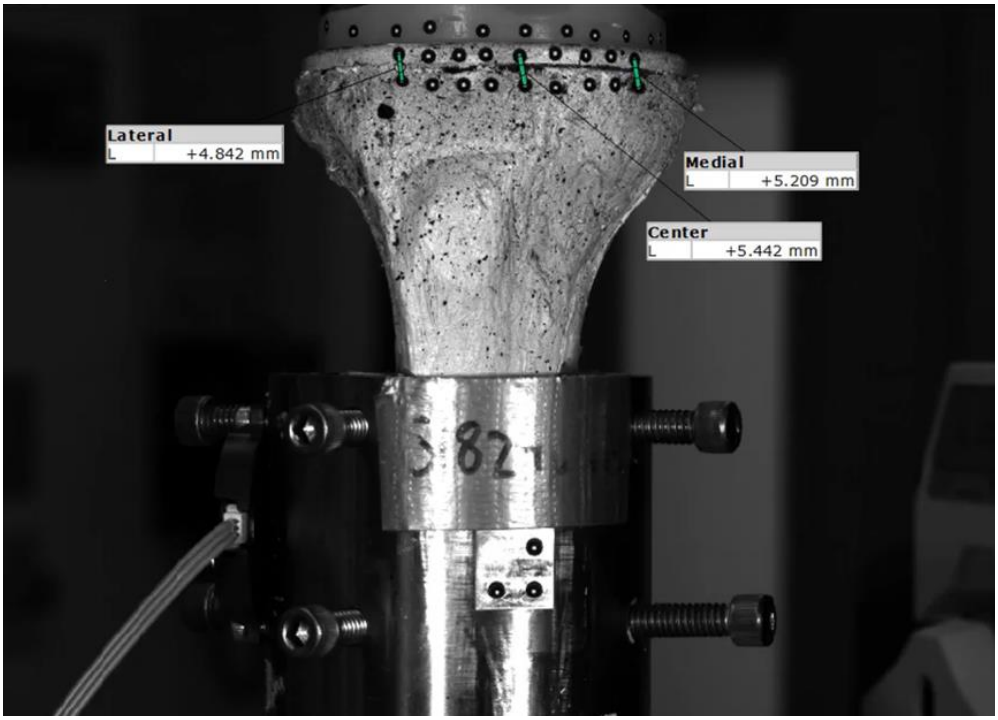

Figure 3.5 Distance between tibial markers

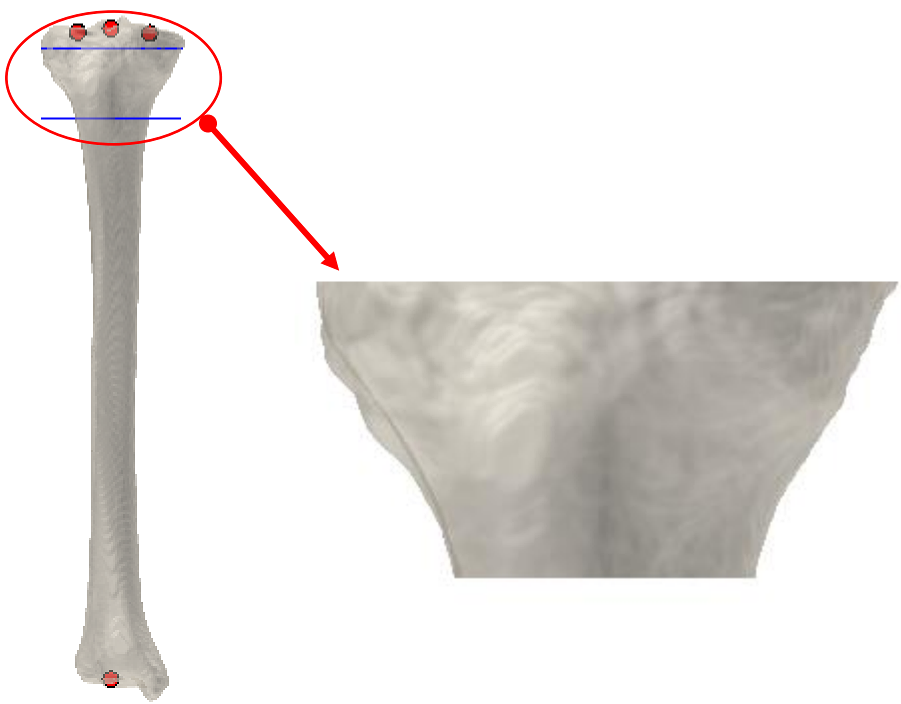

Figure 3.6 Virtual surgery on tibia. Red dots indicate anatomic landmarks to which the tibia was aligned. Blue lines indicate tibial cuts.

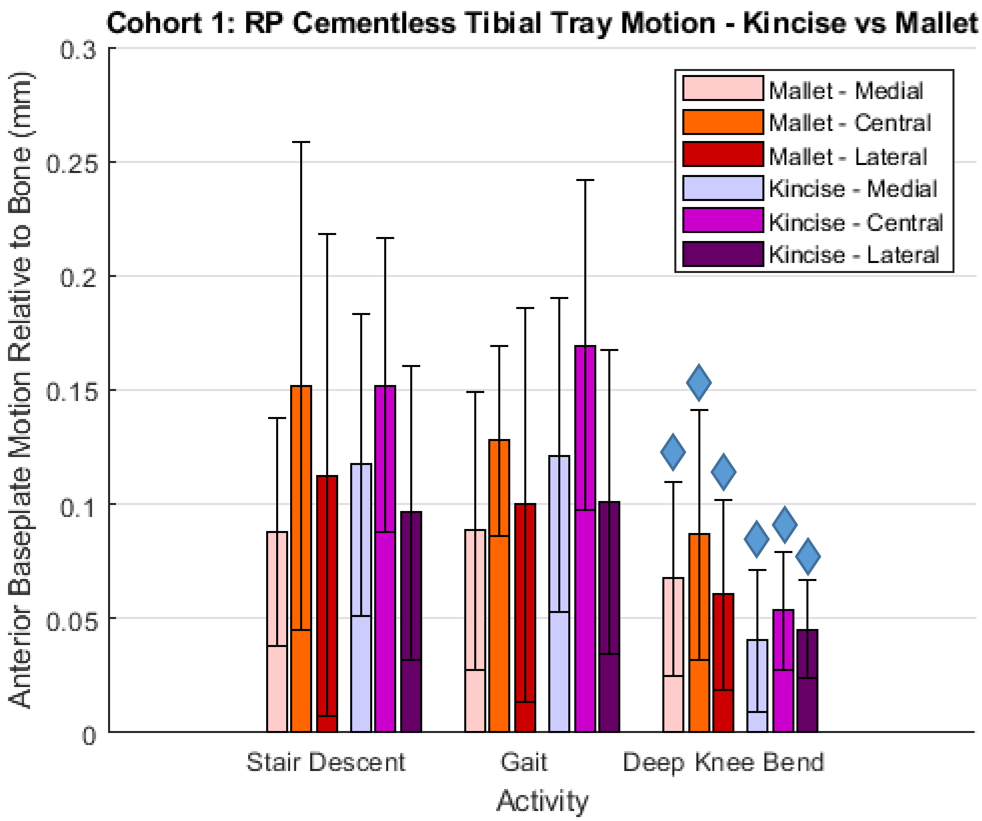

Figure 3.7 Anterior Baseplate Motion Relative to Bone for Cohort 1: Kincise versus Manual Impaction of Attune RP Cementless Tibial Trays. Diamonds indicate statistical significances.

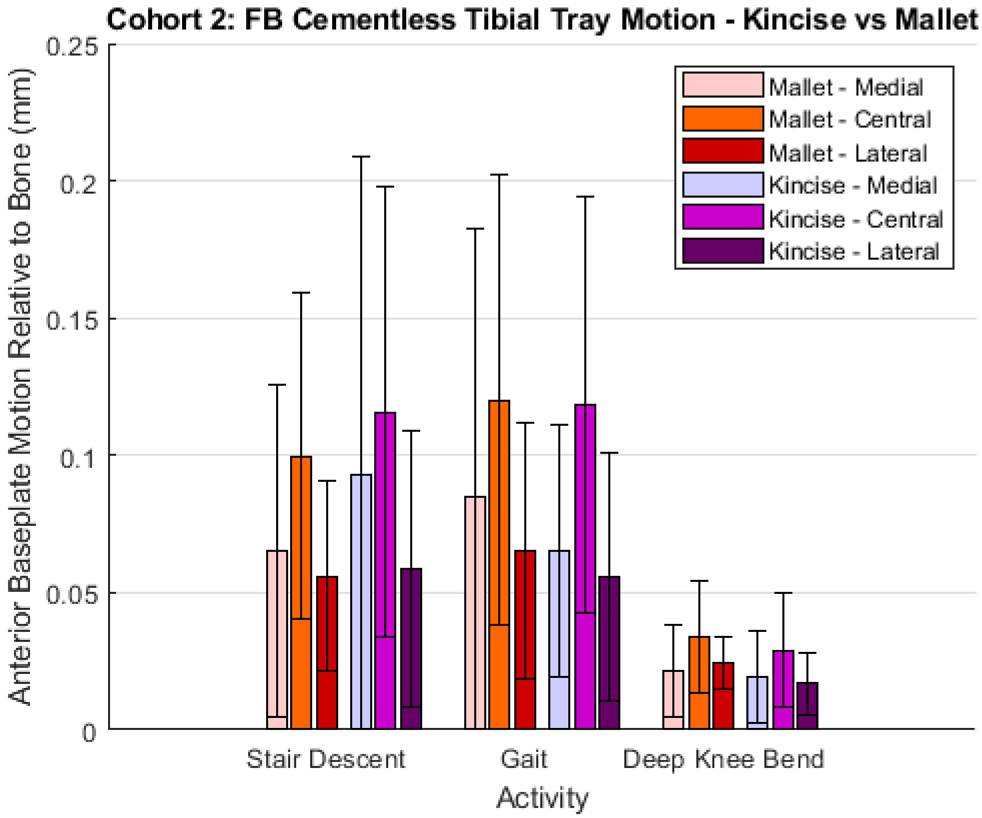

Figure 3.8 Anterior Baseplate Motion Relative to Bone for Cohort 2: Kincise versus Manual Impaction of Attune FB Cementless Tibial Trays

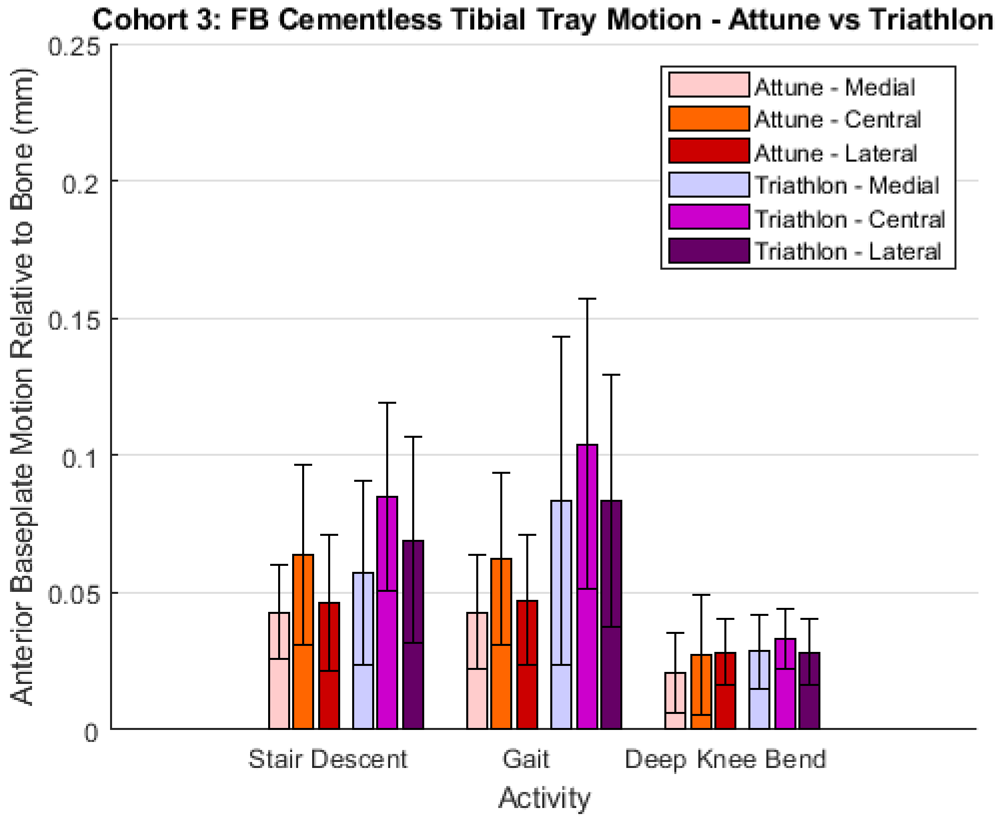

Figure 1.9 Anterior Baseplate Motion Relative to Bone for Cohort 3: Triathlon FB Cementless Tibial Trays versus Attune FB Cementless Tibial Tray

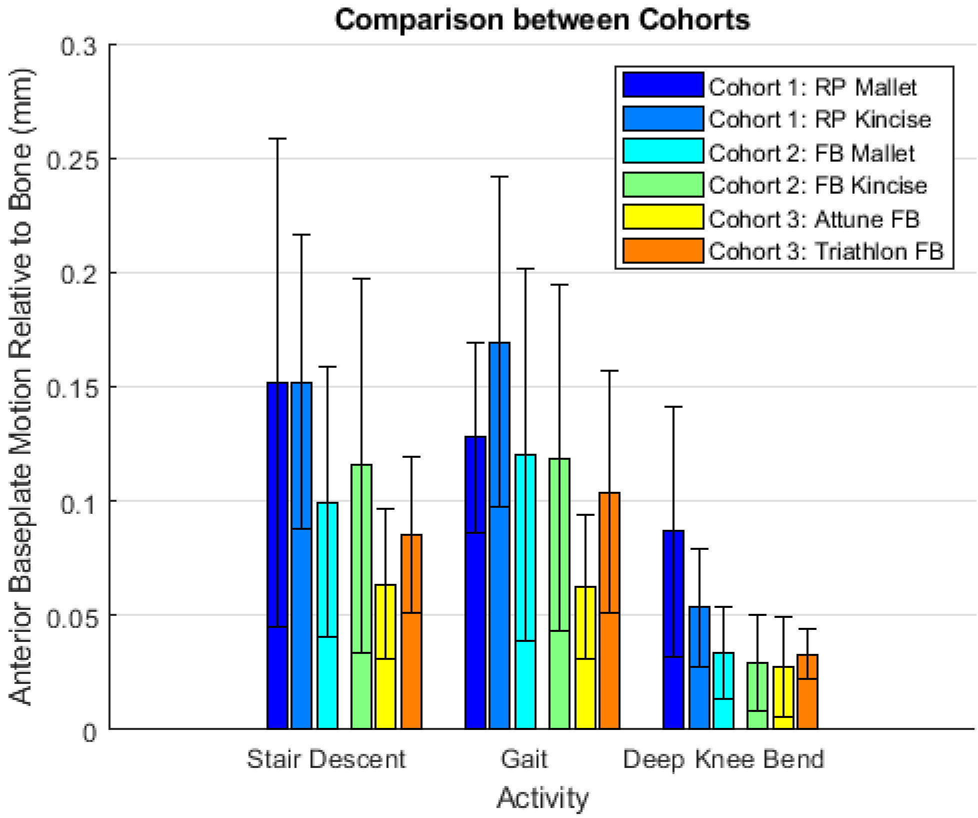

Figure 3.10 Comparison of Anterior Baseplate Motion Relative to Bone between Cohorts for Central marker pairs

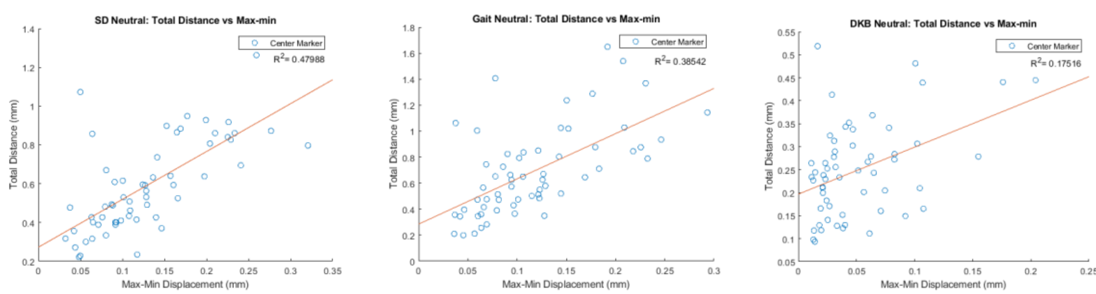

Figure 3.11 Total Distance versus Max-Min Distance for Stair Descent, Gait, and Deep-Knee Bending

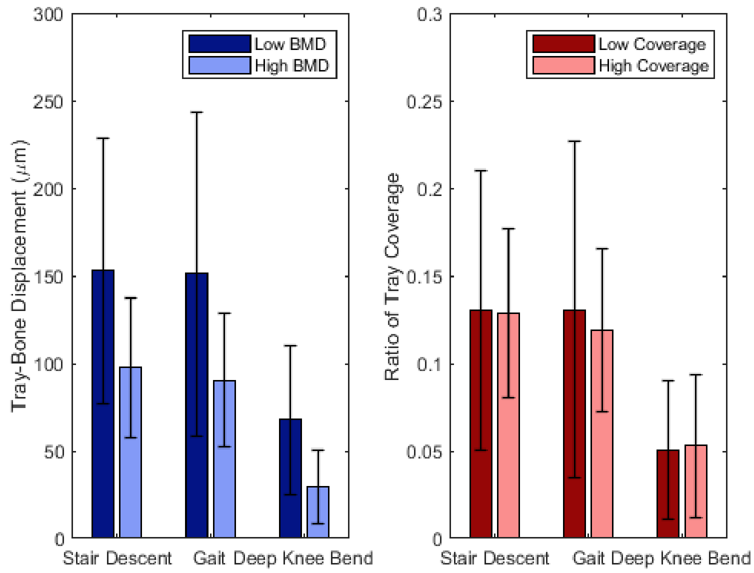

Figure 3.12 Average Tibial Micromotion of Clusters Based on BMD and Tray Coverage

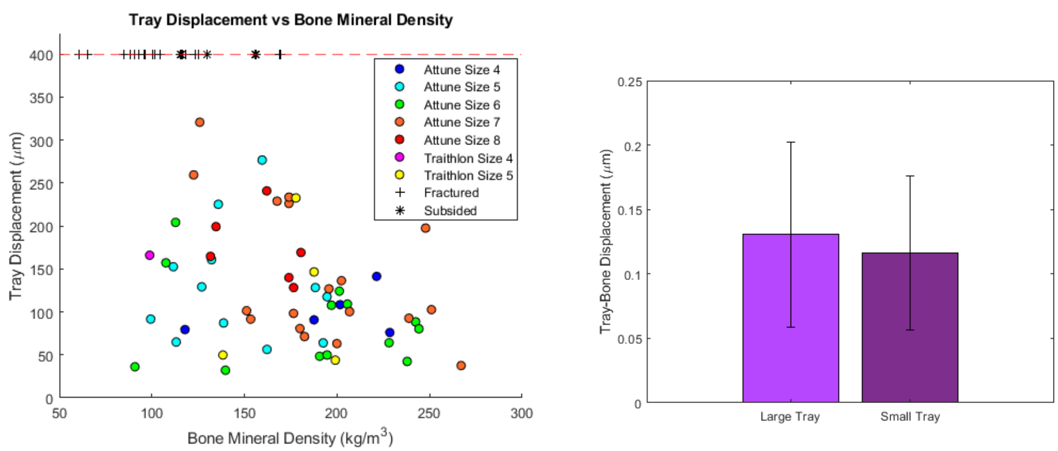

Figure 3.13 Scatter plot of BMD versus Tray Displacement during Stair Descent

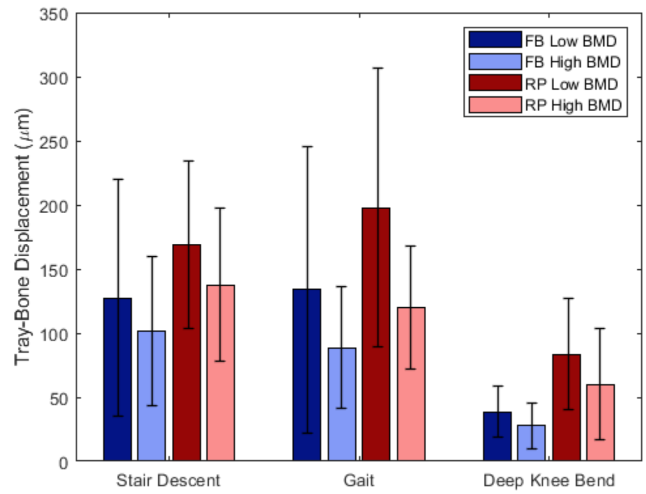

Figure 3.14 Comparison of RP versus FB on Average Tibial Micromotion of Clusters Based on BMD and Tray Coverage

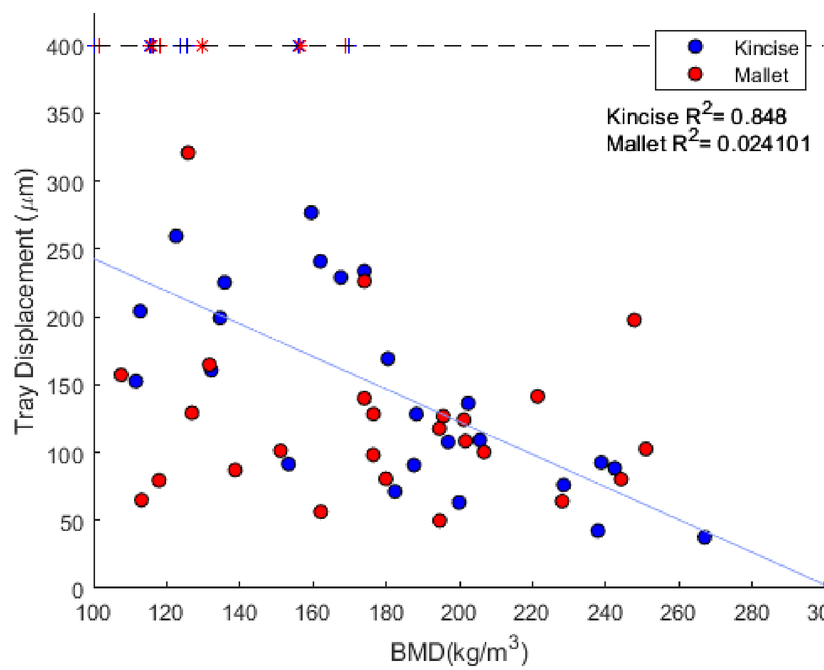

Figure 3.15 Scatter plots of BMD versus Tray Displacement during Stair Descent Separated by Impaction Method

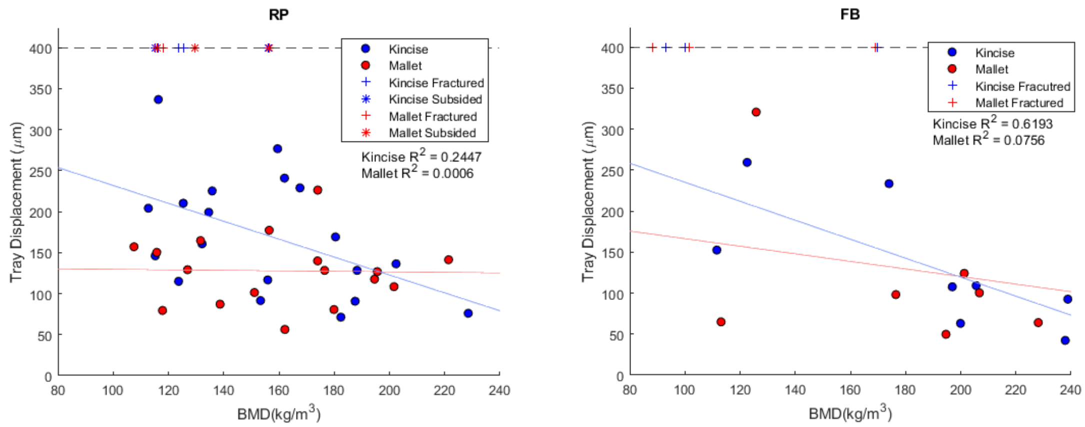

Figure 3.16 Plots of BMD versus Tray-Displacement during Stair Descent Separated by Impaction Method and Implant Type

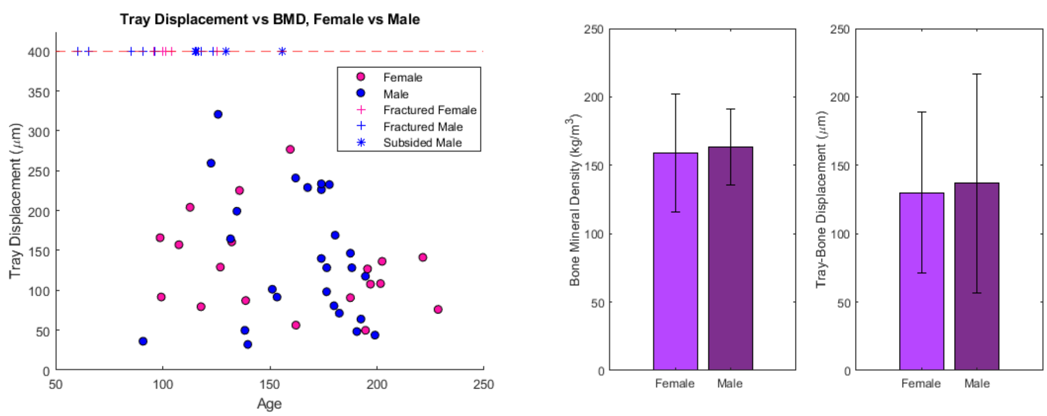

Figure 3.17 Scatter plot of BMD and Tray-bone displacement and barplot grouped by gender

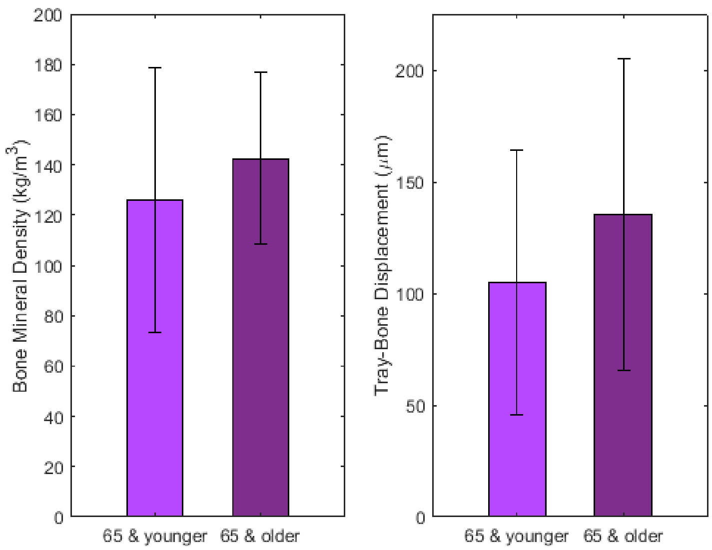

Figure 3.18 Average Tibial Micromotion and BMD of Clusters Based on age

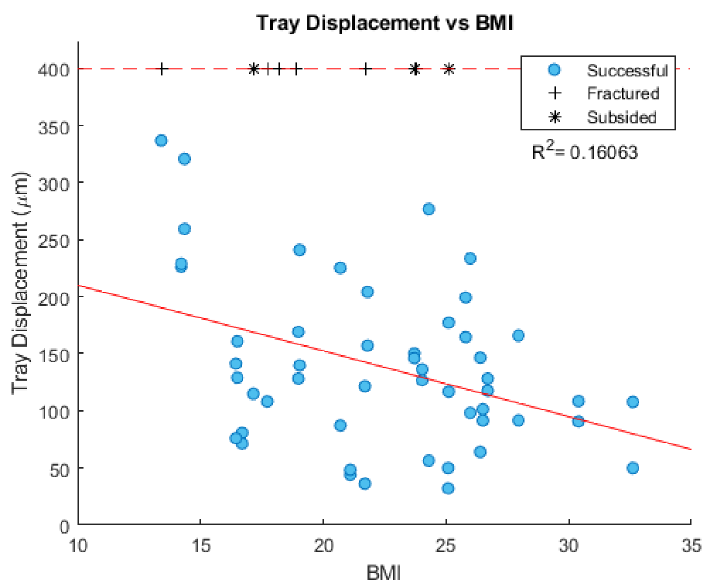

Figure 3.19 Scatter plot of Tray Displacements versus BMI

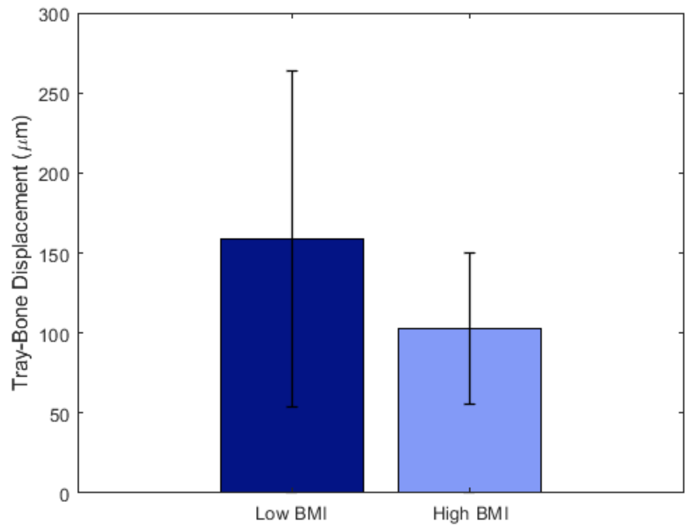

Figure 3.20 Average Tibial Micromotion of Clusters Based on BMI

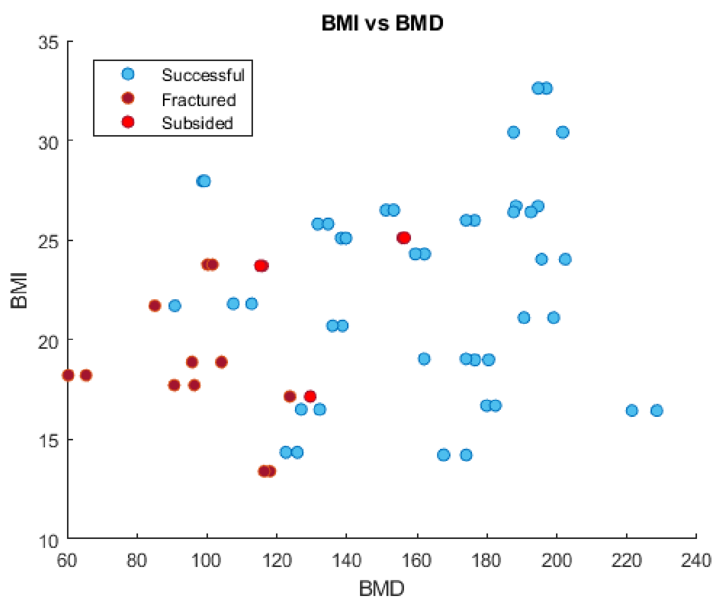

Figure 3.21 Scatter plot for comparison of BMI versus BMD

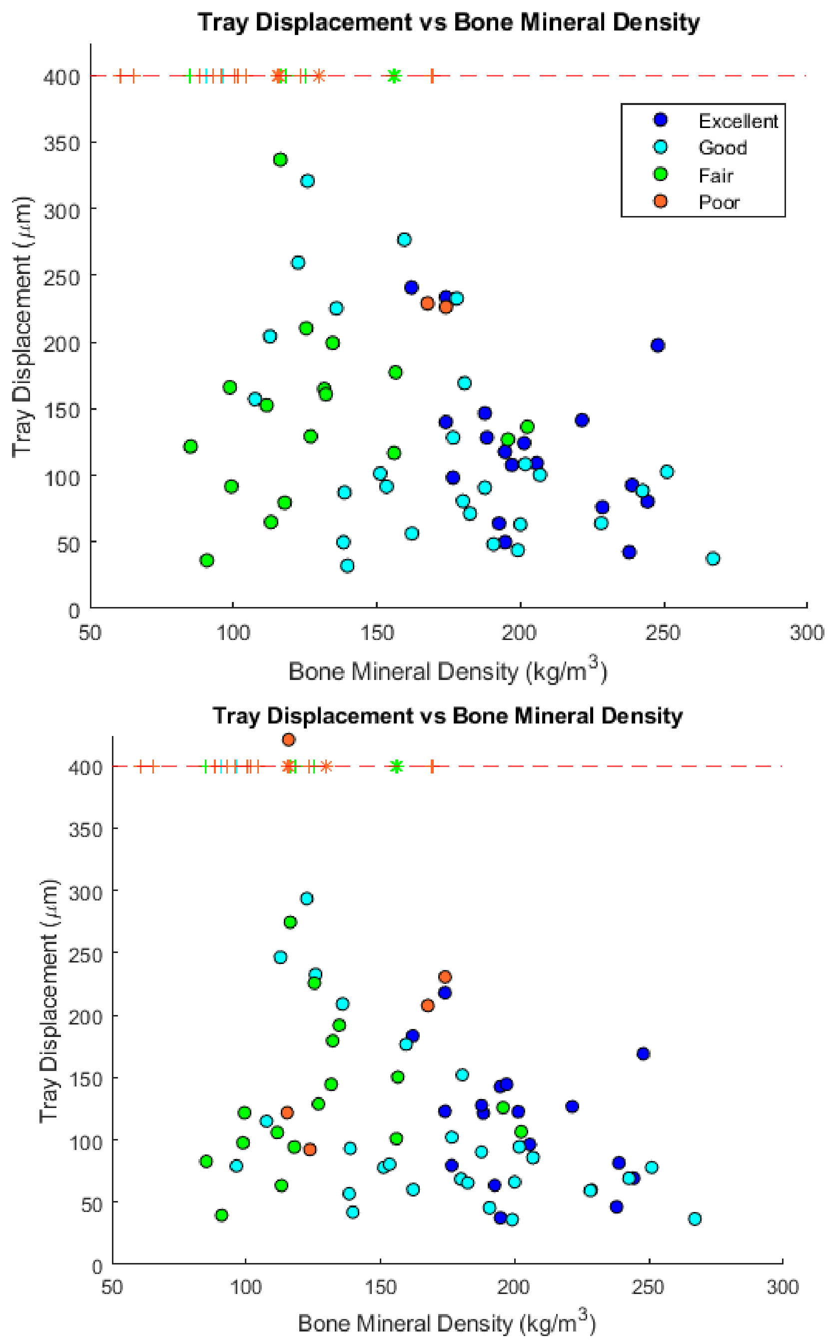

Figure 3.22 Tray Displacement versus BMD with Intraoperative Surgeon Classification of Bone Quality

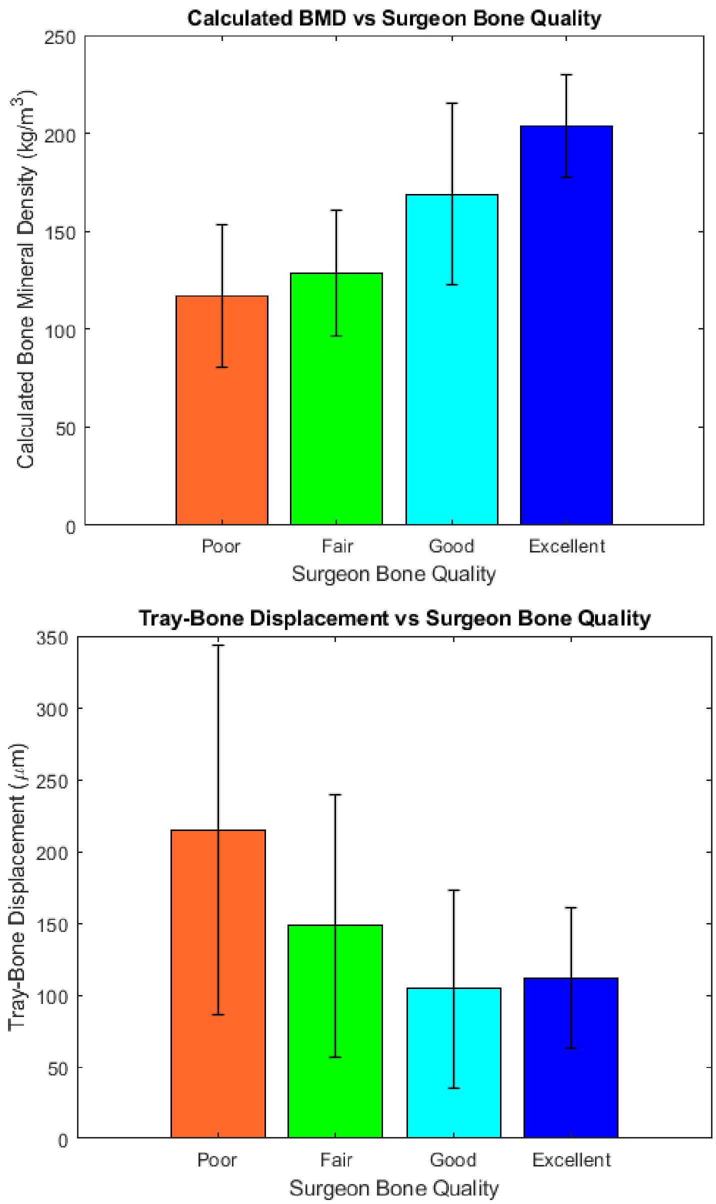

Figure 3.23 Bar Plot of Tray Displacement for Surgeon Classification of Bone Quality

CHAPTER 4. CONCLUSIONS AND RECOMMENDATIONS

4.1 Key Findings

The work presented in this thesis contributes to the orthopaedic research community by advancing knowledge regarding factors effecting initial stability of cementless tibial implants. As the number of younger and more active patients needing TKA's increases, the need for cementless tibial implants increases. Understanding the factors influencing the initial fixation is instrumental to implant success.

As delineated in chapter 2, previous investigations into *in vitro* experimentation of the initial stability of orthopaedic implants and the correlation with bone mineral density have resulted in increased understanding of implant micromotion and characterized the effects of implant design. Early investigations were hindered by limited DOF and lack of investigation into the factors contributing to the initial fixation. The study presented in this thesis addresses shortcomings by utilizing a sophisticated 6-DOF robotic testing rig, multiple loading conditions and an exploration into the effects of initial stability of tibial trays as explained in chapter 3. The most interesting results included the finding that success for each impaction method may be influenced by BMD, BMD overall was a strong contributing factor to increased micromotion or tibial failure and the stronger correlation between BMD and micromotion for Attune RP trays as compared to Attune FB trays, described in chapter 3. Work is currently underway as a result of these findings to modify automated surgical impaction devices so as to improve implant success. A future study will evaluate the influence the flatness of the tibial cut has on micromotion by utilizing a 3D laser scanner on the tibia prior to impaction.

4.2 Limitations and Future Work

This study had several limitations. The placement of the DIC markers was not consistent between specimen, although it was relatively placed in the same location. The distance between corresponding target marker pairs was normalized relative to the unloaded state prior to experimentation. This has the benefit of normalizing the micromotion for each specimen but does not elucidate how the distance between markers has changed relative to the unloaded state after each cycle. As a result, it is difficult to discern whether the motion is due to compressive or tensile loading. Future studies should focus on the changes in tray displacement between activities to note the manner in which the bone is deforming under the various activities. The micromotion was calculated as the maximum minus the minimum displacement. When compared to the total distance traveled, the results differ; however, there is the same general trend for activities. Future studies should focus on the method for calculating micromotion that best expresses how the tray is moving relative to the bone. Additionally, a small sample size was used for the Attune and Triathlon comparison. Future studies should replicate the experiment with a greater sample size to ensure accuracy of results.

Although the testing rig simulates activities using 6-DOF, the simulation is a simplified scenario of actual joint loading without any patient specific attributes. Factors such as BMI and patient anatomy would vary the loads an implant experiences from individual patients. A knee complete with soft tissue would offer more realistic micromotion results for a better comparison between different implant types. Future testing should incorporate the patella and soft tissue structures of the knee to better replicate *in vivo* micromotion results. In addition, the manufacturer specifies that a tibial implant should be two sizes either greater or less than femur implant size. This study utilized the same size 5 femur for all specimen, regardless of tibial implant size. A size five tibial insert was used for all specimen for consistency, but it is unknown whether appropriate femur sizes would vary results. Lastly, we did not quantify if the implant was fully seated nor did we assess the flatness of the tibial cut. Both variables are likely factors influencing initial stability of the cementless implants. Future studies should include these variables when researching factors influencing initial fixation.

BIBLIOGRAPHY

Baldwin, M.A., Clary, C.W., Fitzpatrick, C.K., Deacy, J.S., Maletsky, L.P., Rullkoetter, P.J., 2012. Dynamic finite element knee simulation for evaluation of knee replacement mechanics. J. Biomech. 45, 474–83. https://doi.org/10.1016/j.jbiomech.2011.11.052

Baral, E., Purcel, R., Wright, T., Westrich, G.H., 2020. Bone Ingrowth in Retrieved Porous Coated Tibial Trays. Orthopaedic Proceedings. 102-B:SUPP_1, 91-91.

Basso, T., Klaksvik, J., Syverson, U., Foss, O.A. A biomechanical comparison of composite femurs and cadaver femurs used in experiments on operated hip fractures. Journal of Biomechanics 47 (2014) 3898-3902. https://doi.org/10.1016/j.jbiomech.2014.10.025

Batz, J, Messer-Hannemann, P, Lampe, F, et al. Effect of cavity preparation and bone mineral density on bone-interface densification and bone-implant contact during press-fit implantation of hip stems. J Orthop Res 2019; 37: 1580–1589. https://doiorg.du.idm.oclc.org/10.1002/jor.24288

Bhimani AA, Rizkalla JM, Peters Jr PC, Kitziger KJ, Schubert RD, Gladnick BP. Surgical Automation Reduces Operating Time While Maintaining Accuracy for Direct Anterior Total Hip Arthroplasty. Presented at AAHKS, Dallas Nov 7-10th 2019.

Bhimji, S., Meneghini, R.M., 2014. Micromotion of cementless tibial baseplates: Keels with adjuvant pegs offer more stability than pegs alone. J. Arthroplasty 29, 1503–1506. https://doi.org/10.1016/j.arth.2014.02.016

Bhimji, S., Meneghini, R.M., 2012. Micromotion of Cementless Tibial Baseplates Under Physiological Loading Conditions. J. Arthroplasty 27, 648–654. https://doi.org/10.1016/j.arth.2011.06.010

Bieger R, Ignatius A, Reichel H, Durselen L. Biomechanics of a short stem: In vitro primary stability and stress shielding of a conservative cementless hip stem. J Orthop Res. 2013; 31(8):1180–6. Epub 2013/ 04/05. https://doi.org/10.1002/jor.22349 PMID: 23553802

Chong, D.Y.R., Hansen, U.N., Amis, A.A., 2010. Analysis of bone-prosthesis interface micromotion for cementless tibial prosthesis fixation and the influence of loading conditions. J. Biomech. 43, 1074–1080. https://doi.org/10.1016/j.jbiomech.2009.12.006

Clary, C.W., Fitzpatrick, C.K., Maletsky, L.P., Rullkoetter, P.J., 2013. The influence of total knee arthroplasty geometry on mid-flexion stability: An experimental and finite element study. J. Biomech. 46, 1351–1357. https://doi.org/10.1016/j.jbiomech.2013.01.025

Cohen, R. G., Sherman, N. C., & James, S. L. (2018). Early clinical outcomes of a new cementless total knee arthroplasty design. Orthopedics, 41(6), 765-771. http://dx.doi.org.du.idm.oclc.org/10.3928/01477447-20180828-05

Crook, P.D., Owen, J.R., Hess, S.R., Al-Humadi, S.M., Wayne, J.S., Jiranek, W.A., 2017. Initial Stability of Cemented vs Cementless Tibial Components Under Cyclic Load. J. Arthroplasty 32, 2556–2562. https://doi.org/10.1016/j.arth.2017.03.039

Favre, P., Seebeck, J., Thistlethwaite, P.A., Obrist, M., Steffens, J.G., Hopkins, A.R., Hulme, P.A., 2016. In vitro initial stability of a stemless humeral implant. Clin. Biomech, 32, 113-7. https://doi.org/10.1016/j.clinbiomech.2015.12.004

Fitzpatrick, C.K., Baldwin, M.A., Clary, C.W., Maletsky, L.P., Rullkoetter, P.J. Evaluating knee replacement mechanics during ADL with PID-controlled dynamic finite element analysis. Comput Methods Biomech Biomed Engin. 2014;17(4):360-9.

Fitzpatrick, C.K., Maag, C., Clary, C.W., Metcalfe, A., Langhorn, J., Rullkoetter, P.J., 2016. Validation of a new computational 6-DOF knee simulator during dynamic activities. J. Biomech. 49, 3177–3184.https://doi.org/10.1016/j.jbiomech.2016.07.040

Gargiulo, P., Petursson, T., Magnusson, B., 2013. Assessment of total hip arthroplasty by means of computed tomography 3D models and fracture risk evaluation. Artificial Organs, 37, 567–573.

Gebert, A., Peters, J., Bishop, N. E., Westphal, F., Morlock, M. M., 2009. Influence of press fit parameters on the primary stability of uncemented femoral resurfacing implants. Med Eng Phys. 31(1), 160–164. https://doi.org/10.1016/j.medengphy.2008.04.007

Haider, H., Walker, P.S., 2005. Measurements of constraint of total knee replacement. J. Biomech. 38, 341-348. https://doi.org/10.1016/j.jbiomech.2004.02.014

Hofmann, A.A., Bloebaum, R.D., Bachus, K.N. Progression of human bone ingrowth into porous-coated implants: Rate of bone ingrowth in humans. Acta Orthopaedica Scandinavica, 68:2, 161-166, DOI: 10.3109/17453679709004000=

Jun Ito, Tomihisa Koshino, Renzo Okamoto, Tomoyuki Saito, 15-year follow-up study of total knee arthroplasty in patients with rheumatoid arthritis, The Journal of Arthroplasty, Volume 18, Issue 8, 2003, Pages 984-992, ISSN 0883-5403, http://dx.doi.org/10.1016/S0883-5403(03)00262-6.

Kerkhoffs, G.M., Servien, E., Dunn, W., Dahm, D., Bramer, J.A., & Haverkamp, D. The influence of obesity on the complication rate and outcome of total knee arthroplasty: a meta-analysis and systematic literature review. J Bone Joint Surg Am. 2012;94(20):1839-1844. doi:10.2106/JBJS.K.00820

Kurtz, S.M., Lau, E., Ong, K., Zhao, K., Kelly, M., & Bozic, K.J. Future young patient demand for primary and revision joint replacement: national projections from 2010 to 2030. Clinical Orthopedics and Related Research, 467 (2009), pp. 2606-2612

McCalden, R.W., Robert, C.E., Howard, J.L., Naudie, D.D., McAuley, J.P., & MacDonald, S.J. Comparison of outcomes and survivorship between patients of different age group following TKA. J. Arthro, 28 (Suppl. 8) (2013), pp. 83-86

Meek RM, Norwood T, Smith R, Brenkel IJ, Howie CR: The risk of peri-prosthetic fracture after primary and revision total hip and knee replacement. J. Bone Joint Surg Br 2011;93:96-101. https://doi.org/10.1302/0301-620X.93B1.25087

Nadorf J, Thomsen M, Gantz S, Sonntag R, Kretzer JP. Fixation of the shorter cementless GTS stem: biomechanical comparison between a conventional and an innovative implant design. Arch Orthop Trauma Surg. 2014; 134(5):719–26. Epub 2014/02/14. https://doi.org/10.1007/s00402-014-1946-3 PMID: 24522862

Magnusson, B., Petursson, P., Edmunds, K., 2015. Improving planning and post-operative assessment for total hip arthroplasty, European Journal of Translational Myology—Basic Applied Myology, 25, 101–108.

Marquezan, M., Osório, A., Sant’Anna, E., Souza, M.M., Maia, L., 2012. Does bone mineral density influence the primary stability of dental implants? A systematic review.Clin. Oral Impl. Res . 23, 767–774. doi: 10.1111/j.1600-0501.2011.02228.x

Pal, B., Gupta, S., New, A.M., Browne, M., (2010). Strain and micromotion in intact and resurfaced composite femurs: experimental and numerical investigations. J. Biomech. 43(10):1923–30. Epub 2010/04/16. https://doi.org/10.1016/j.jbiomech.2010.03.019 PMID: 20392448 27.

Pétursson, Þ., Edmunds, K.J., Gíslason, M.K., Magnússon, B., Magnúsdóttir, G., Halldórsson, G., Jónsson, H., Gargiulo, P., 2015. Bone Mineral Density and Fracture Risk Assessment to Optimize Prosthesis Selection in Total Hip Replacement. Computational and Mathematical Methods in Medicine, 1–7. doi:10.1155/2015/162481

Sloan, M.,Premkumar, A., Sheth, N., Projected Volume of Primary Total Joint Arthroplasty in the U.S., 2014 to 2030, The Journal of Bone and Joint Surgery: September 5, 2018 - Volume 100 - Issue 17 - p 1455-1460. doi: 10.2106/JBJS.17.01617

Small, S.R., Rogge, R.D., Malinzak, R.A., Reyes, E.M., Cook, P.L., Farley, K.A., & Ritter, M.A. (2016). Micromotion at the tibial plateau in primary and revision total knee arthroplasty: fixed versus rotating platform designs. Bone & joint research, 5(4), 122–129. https://doi.org/10.1302/2046-3758.54.2000481

Walsh, C.P., Han, S., Cahjam, C.D., Gonzalez, J.L.,, Noble, P., Incavo, S.J., 2019. Total Knee Arthoplasty in the Osteoporotic Tibia: A Biomechanical Evaluation of the Role of Stem Extensions and Cementing Techniques. J. Am Acad Orthop Surg. 27(10), 370-374. https://doi.org/10.5435/JAAOS-D-17-00736

Weiser, L., Huber, G., Sellenschloh, K., Viezens, L., Klaus, P., Morlock, M. M., Lehmann, W., 2017. Insufficient stability of pedicle screws in osteoporotic vertebrae: biomechanical correlation of bone mineral density and pedicle screw fixation strength. Eur Spine J 26, 2891–2897. https://doi-org.du.idm.oclc.org/10.1007/s00586-017-5091-x